

Dijet production in $\sqrt{s} = 7$ TeV pp collisions with large rapidity gaps at the ATLAS experiment



ATLAS Collaboration ^{*}

ARTICLE INFO

Article history:

Received 3 November 2015

Received in revised form 10 January 2016

Accepted 15 January 2016

Available online 18 January 2016

Editor: W.-D. Schlatter

ABSTRACT

A 6.8 nb^{-1} sample of pp collision data collected under low-luminosity conditions at $\sqrt{s} = 7$ TeV by the ATLAS detector at the Large Hadron Collider is used to study diffractive dijet production. Events containing at least two jets with $p_T > 20$ GeV are selected and analysed in terms of variables which discriminate between diffractive and non-diffractive processes. Cross sections are measured differentially in $\Delta\eta^F$, the size of the observable forward region of pseudorapidity which is devoid of hadronic activity, and in an estimator, $\tilde{\xi}$, of the fractional momentum loss of the proton assuming single diffractive dissociation ($pp \rightarrow pX$). Model comparisons indicate a dominant non-diffractive contribution up to moderately large $\Delta\eta^F$ and small $\tilde{\xi}$, with a diffractive contribution which is significant at the highest $\Delta\eta^F$ and the lowest $\tilde{\xi}$. The rapidity-gap survival probability is estimated from comparisons of the data in this latter region with predictions based on diffractive parton distribution functions.

© 2016 CERN for the benefit of the ATLAS Collaboration. Published by Elsevier B.V. This is an open access article under the CC BY license (<http://creativecommons.org/licenses/by/4.0/>). Funded by SCOAP³.

1. Introduction

Diffractive dissociation (e.g. $pp \rightarrow pX$) contributes a large fraction of the total inelastic cross section [1] at the Large Hadron Collider (LHC). The inclusive process has been studied using the earliest LHC data in samples of events in which a large gap is identified in the rapidity distribution of final-state hadrons [2,3]. In the absence of hard scales, the understanding of these data is based on phenomenological methods rather than the established theory of the strong interaction, quantum chromodynamics (QCD).

A subset of diffractive dissociation events in which hadronic jets are produced as components of the dissociation system, X , was first observed at the SPS [4], a phenomenon which has since been studied extensively at HERA [5,6] and the Tevatron [7]. The jet transverse momentum provides a natural hard scale for perturbative QCD calculations, making the process sensitive to the underlying parton dynamics of diffraction and colour-singlet exchange. A model [8] in which the hard scattering is factorised from a colourless component of the proton with its own partonic content (diffractive parton distribution functions, DPDFs), corresponding to the older concept of a pomeron [9], has been successful in describing diffractive deep inelastic scattering ($ep \rightarrow eXp$) at HERA [10]. The DPDFs have been extracted from fits to HERA data in the framework of next-to-leading-order QCD, revealing a highly gluon-dominated structure [11,12].

The success of the factorisable approach breaks down when DPDFs from ep scattering are applied to hard diffractive cross sections in photoproduction [13,14] or at hadron colliders. Tevatron data [7] show a suppression of the measured cross section by a factor of typically 10 relative to predictions. A similar ‘rapidity-gap survival probability’ factor, usually denoted by S^2 , was suggested by the first results from the LHC [15]. This factorisation breaking is usually attributed to secondary scattering from beam remnants, also referred to as absorptive corrections, and closely related to the multiple-scattering effects which are a primary focus of underlying-event studies [16–18]. Understanding these effects more deeply is an important step towards a complete model of diffractive processes at hadronic colliders and may point the way towards a reconciliation of the currently very different theoretical treatments of soft and hard strong interactions.

In this paper, the ATLAS technique for finding large rapidity gaps, first introduced in Ref. [2], is developed further and applied to events in which a pair of high transverse momentum (p_T) jets is identified. The resulting cross sections are measured as a function of the size of the rapidity gap and of an estimator of the fractional energy loss of the intact proton. The results are interpreted through comparisons with Monte Carlo models which incorporate DPDF-based predictions with no modelling of multiple scattering. Comparisons between the measurements and the predictions thus provide estimates of the rapidity-gap survival probability applicable to single dissociation processes at LHC energies.

^{*} E-mail address: atlas.publications@cern.ch.

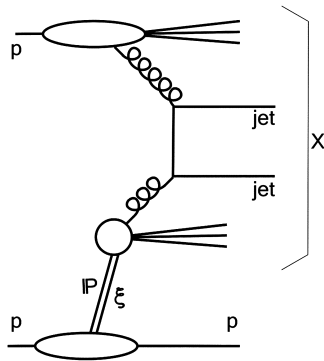


Fig. 1. Illustration of hard single-diffractive scattering, in which partons from a pomeron (\mathbb{P}) and from a proton enter a hard sub-process. The rapidity gap appears between the system X and the intact proton.

2. Models and simulations

Monte Carlo (MC) simulations using leading-order (LO) calculations in perturbative QCD are used in unfolding the data to correct for experimental effects and in the comparison of the measurements with theoretical models. The PYTHIA 8.165 (hereafter referred to as PYTHIA8) general-purpose LO MC generator [19] is used to model dijet production in non-diffractive (ND) events, as well as in single diffractive dissociation (SD, $pp \rightarrow Xp$) and double diffractive dissociation (DD, $pp \rightarrow XY$). An alternative model of the SD process is provided by POMWIG (version 2.0 β) [20], whilst an alternative next-to-leading-order (NLO) model of the ND process is provided by POWHEG (version 1.0) [21,22].

In both PYTHIA8 and POMWIG, hard scattering in diffractive processes takes place through the factorisable pomeron mechanism [8] illustrated in Fig. 1. A pomeron couples to an incoming proton, acquiring a fraction ξ of the proton's longitudinal momentum. The proton either scatters elastically (SD) or dissociates to form a higher-mass system (DD). A parton from the pomeron (as described by DPDFs) then undergoes a hard scattering with a parton from the dissociating proton at a scale set by the transverse momenta of the resulting jets. The dissociation system X has an invariant mass M_X , such that $\xi = M_X^2/s$ at a proton-proton centre-of-mass energy \sqrt{s} .

POMWIG is based on a standard implementation of hard diffractive scattering with a factorisable pomeron, in which both the pomeron flux and the DPDFs are taken from the results of the H1 2006 DPDF fit B¹ [11] and the proton PDF set is CTEQ61 [23]. In contrast, PYTHIA8 provides a simultaneous model of hard and soft diffraction [24], in which a soft diffractive model inherited from PYTHIA6 [25] is smoothly interfaced to a hard diffractive model similar to that in POMWIG. The probability of using the hard model depends on M_X . The H1 2006 DPDF fit B is again used for the partonic content of the pomeron and the proton partonic structure is taken from the CT10 PDFs [26]. Several different pomeron flux parameterisations are available in PYTHIA8. In addition to the default Schuler and Sjöstrand (S-S) model [27], alternative parameterisations by Donnachie and Landshoff (D-L) [28] and Berger and Streng [29,30], as well as the Minimum Bias Rockefeller (MBR) model [31], are also considered in this analysis. These models differ primarily in their predictions for the ξ dependence of the cross section [24]. The DD process in PYTHIA8 is modelled similarly to the SD process. Neither of the diffractive models con-

sidered here take rapidity-gap destruction effects into account, i.e. they set the rapidity gap survival probability $S^2 \equiv 1$.

An alternative for ND processes is provided by the POWHEG NLO generator. As described in Ref. [22], the ‘hardest emission cross section’ approach used in POWHEG avoids the pathological behaviour observed in calculating cross sections with symmetric jet cuts in fixed-order NLO calculations. Here, NLO dijet production in the DGLAP formalism is interfaced with PYTHIA 8 to resum soft and collinear emissions using the parton shower approximation.

PYTHIA8 adopts the Lund String model [32] for hadronisation in each of the ND, SD and DD channels. It also contains an underlying-event model based on multiple parton interactions (MPI). POMWIG is derived from HERWIG [33] and thus inherits its fragmentation and cluster-based hadronisation models. For the purposes of this paper, the POWHEG ND simulation is interfaced to PYTHIA8 for fragmentation and hadronisation. All considered models based on the PYTHIA hadronisation model include p_T -ordered parton showering, while those based on HERWIG use angular-ordered parton showering.

The default MC combination used for the data unfolding for detector effects is a mixture of PYTHIA8 samples of ND, SD and DD dijets, with the ‘ATLAS AU2-CT10’ set of tuned parameters (tune) [34] for the underlying event. In this tune, the fraction of the total cross section attributed to the SD process is reduced relative to the default by 10% and that to DD by 12%, to better match early LHC data. The Berger–Streng parameterisation, which has a very similar ξ dependence to D–L, is chosen for the pomeron flux factor. Finally, the interaction of the particles with the ATLAS detector is simulated using a GEANT4-based program [35,36].

3. The ATLAS detector

The ATLAS detector is described in detail elsewhere [37]. The beam-line is surrounded by a tracking system, which covers the pseudorapidity² range $|\eta| < 2.5$, consists of silicon pixel, silicon strip and straw tube detectors and is immersed in the 2 T axial magnetic field of a superconducting solenoid. The calorimeters lie outside the tracking system. A highly segmented electromagnetic (EM) liquid-argon sampling calorimeter covers the range $|\eta| < 3.2$. The EM calorimeter also includes a presampler covering $|\eta| < 1.8$. The hadronic end-cap (HEC, $1.5 < |\eta| < 3.2$) and forward (FCAL, $3.1 < |\eta| < 4.9$) calorimeters also use liquid argon for their sensitive layers, but with reduced granularity. Hadronic energy in the central region is reconstructed in a steel/scintillator-tile calorimeter. The shapes of the cell noise distributions in the calorimeters are well described by Gaussian distributions, with the exception of the tile calorimeter, where the noise has extended tails, and which is thus excluded from the rapidity gap finding aspects of the analysis. Minimum-bias trigger scintillator (MBTS) detectors are mounted in front of the end-cap calorimeters on both sides of the interaction point and cover the pseudorapidity range $2.1 < |\eta| < 3.8$. The MBTS is divided into inner and outer rings, both of which have eight-fold segmentation. In the analysis, two trigger systems are used at Level-1 (L1), namely the MBTS which efficiently collects low- p_T jets, and the calorimeter-based trigger (L1Calo) which concentrates on higher- p_T jets. In 2010, the luminosity was measured by monitoring the activity in forward detector components, with calibration determined through van der Meer beam scans [38,39].

¹ The H1 Fit B DPDFs correspond to the sum of the SD process and the component of the DD process where the lower of the two proton dissociation masses is smaller than 1.6 GeV (see Section 6).

² In the ATLAS coordinate system, the z -axis points in the direction of the anti-clockwise beam viewed from above. Polar angles θ and transverse momenta p_T are measured with respect to this axis. The pseudorapidity $\eta = -\ln \tan(\theta/2)$ is a good approximation to the rapidity of a particle whose mass is negligible compared with its energy and is used here, relative to the nominal $z = 0$ point at the centre of the apparatus, to describe regions of the detector.

4. Experimental method

To study rapidity-gap production, the experiment needs to operate at very low luminosities such that there is on average much less than one collision per bunch crossing (i.e. negligible ‘pile-up’). This requirement has to be balanced against the need to collect adequate numbers of events with large rapidity gaps. The analysis therefore uses data from an early 2010 LHC run, with a total integrated luminosity of 6.8 nb^{-1} . The average number of collisions per bunch crossing is 0.12.

The jet selection follows that used in the ATLAS 2010 dijet analysis [40]. Jets with $p_T > 20 \text{ GeV}$ and $|\eta| < 4.4$ are reconstructed by applying the anti- k_t algorithm [41] to topological clusters at the standard ATLAS jet energy scale. For comparisons, in particle-level MC models, jets are formed with the anti- k_t algorithm from stable ($c\tau > 10 \text{ mm}$) final-state particles. The analysis is performed with jets of two different radius parameters $R = 0.4$ and $R = 0.6$. Approximately twice as many jets are reconstructed with the $R = 0.6$ than with the $R = 0.4$ requirement in the kinematic range covered here.

The calorimeter-based jet trigger (‘L1Calo’) is used with the lowest available p_T threshold in phase-space regions where its efficiency is determined to be greater than 60%. This criterion is satisfied for central jets at all pseudorapidities in the range $|\eta| < 2.9$ with $p_T > 29$ (34) GeV for jets with $R = 0.4$ (0.6). At lower transverse momenta, or where the jets are beyond the L1Calo η range, the MBTS trigger is used, with the requirement of a signal in at least one segment. The MBTS trigger is fully efficient for dijet events, but has a substantial time-dependent prescale (which is taken into account in the off-line analysis), reducing the effective luminosity for forward and low- p_T jets to 0.303 nb^{-1} .

At least two jets are required, with jet barycentres satisfying $|\eta| < 4.4$ and with $p_T > 20 \text{ GeV}$. These requirements correspond to the region in which the jet energy scale and resolution are well known and in which the jets are fully contained within the detector.

Several sources of background were investigated. To reject contributions from beam interactions with residual gas in the beampipe, muons from upstream proton interactions travelling as a halo around the proton beam, and cosmic-ray muons, events are required to have a primary vertex constructed from at least two tracks and consistent with the beam spot position. In-time pile-up, caused by multiple interactions in one bunch crossing, is suppressed by requiring that there be no further vertices with two or more associated tracks. Out-of-time pile-up, caused by overlapping signals in the detector from neighbouring bunch crossings, was investigated and found to be negligible at the large bunch spacings ($> 5 \mu\text{s}$) of the chosen runs. Once an event is triggered and the dijet selection criteria are met, the requirement on the primary vertex removes 0.3% and 0.2% of events in the L1Calo- and MBTS-triggered data, respectively, while the in-time pile-up suppression cuts remove 9.4% and 6.5%, respectively. The latter values are used to scale the cross sections to account for the corresponding losses. Residual background occurs due to the limited position resolution of the vertex reconstruction, which typically merges pairs of vertices with $\Delta z \lesssim 1 \text{ cm}$ into a single vertex. The size of this effect is estimated by extrapolation to lower values of the Δz distribution for pairs of vertices which are resolved and its influence is evaluated by randomly overlaying minimum-bias events on the selected sample. The effect is smaller than 0.5% in all bins of the measured distributions. The residual beam-induced background is studied using ‘unpaired’ bunch crossings in which only one bunch of protons passes through the ATLAS detector and is found to be negligible.

Each event is characterised in terms of pseudorapidity regions which are devoid of hadronic activity (‘rapidity gaps’) using a method very similar to that first introduced in Ref. [2]. Rapidity gaps are defined using the tracking ($|\eta| < 2.5$ and $p_T > 200 \text{ MeV}$) and calorimetric ($|\eta| < 4.8$) information within the ATLAS detector acceptance. Full details of the track selection can be found in Ref. [42]. Following Ref. [2], the clustering algorithm accepts calorimeter cells as cluster seeds if their measured response is approximately five standard deviations above the root-mean-square noise level, with a small dependence of the threshold on pseudorapidity. Cells neighbouring the seed cell are included in the cluster if their measured energies exceed smaller threshold requirements defined by the standard ATLAS topological clustering method. The particle-level gap definition is determined by the region of pseudorapidity with an absence of neutral particles with $p > 200 \text{ MeV}$ and charged particles with either $p > 500 \text{ MeV}$ or $p_T > 200 \text{ MeV}$. These momentum and transverse momentum requirements match the ranges over which the simulation indicates that particles are likely to be recorded in the detectors, accounting for the axial magnetic field in the inner detector. The treatment of calorimeter information in the rapidity-gap determination follows the procedure introduced in Ref. [43], such that the requirement $p_T > 200 \text{ MeV}$ for calorimeter clusters from the previous rapidity-gap analysis [2] is removed. Since this transverse momentum requirement corresponds to a very high momentum at large pseudorapidities, the modified approach more completely exploits the capabilities of ATLAS to detect low-momentum particles in the calorimeters. The total numbers of selected events in the L1Calo and MBTS samples with $R = 0.6$ are 285 191 and 44 372, respectively.

The variable characterising forward rapidity gaps, $\Delta\eta^F$, is defined by the larger of the two empty pseudorapidity regions extending between the edges of the detector acceptance at $\eta = 4.8$ or $\eta = -4.8$ and the nearest track or calorimeter cluster passing the selection requirements at smaller $|\eta|$. No requirements are placed on particle production at $|\eta| > 4.8$ and no attempt is made to identify gaps in the central region of the detector. In this analysis, the size of the rapidity gap relative to $\eta = \pm 4.8$ lies in the range $0 < \Delta\eta^F < 6.5$. For example $\Delta\eta^F = 6.5$ implies that there is no reconstructed particle with (transverse) momentum above threshold in one of the regions $-4.8 < \eta < 1.7$ or $-1.7 < \eta < 4.8$.

For events which are of diffractive origin, the Monte Carlo studies indicate that the rapidity-gap definition selects processes in which one of the incoming protons either remains intact (SD) or is excited to produce a system with mass $M < 7 \text{ GeV}$ (DD). In the second case, the system is typically restricted to a pseudorapidity region beyond the acceptance of the ATLAS detector. In both cases, the other incoming proton dissociates to produce a hadronic system of larger invariant mass M_X . The gap size, $\Delta\eta^F$, grows approximately logarithmically with $1/M_X$, the degree of correlation being limited by event-to-event hadronisation fluctuations.

In this analysis, measurements of the energy deposits in each event are used to construct a variable, $\tilde{\xi}$ which is closely correlated with ξ and is similar to that used in Ref. [15]. Neglecting any overall transverse momentum of the system X , the relation

$$M_X^2 = \sqrt{s} \sum p_T e^{\pm\eta}, \quad (1)$$

holds for cases where the intact proton travels in the $\pm z$ direction. In other words, if the forward rapidity gap starts at $\eta = +4.8$ (-4.8), the exponential function takes the positive (negative) sign. Here, the sum runs over all particles constituting the system X . This relation has the attractive feature that the sum is relatively insensitive to particles in the X system travelling in the very forward direction, i.e. those which are produced at large

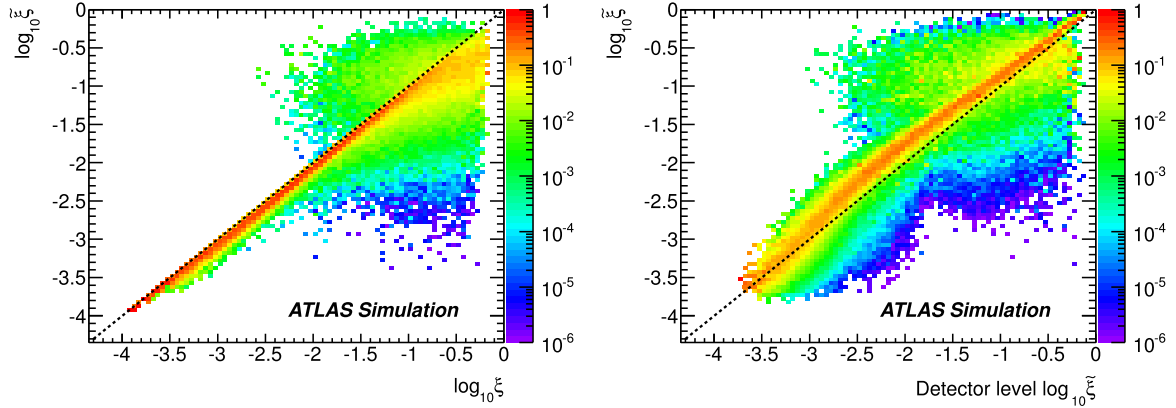


Fig. 2. (a) Particle-level correlation between the ξ variable extracted from the diffractively scattered proton and $\tilde{\xi}$ calculated from particles selected as defined in the text, using the PYTHIA8 SD MC model. (b) Correlation between the particle-level $\tilde{\xi}$ and detector-level $\tilde{\xi}$ calculated from clusters selected as defined in the text, using the sum of PYTHIA8 ND, SD and DD contributions. In both plots, the distributions are normalised to unity in each column.

pseudorapidities beyond the detector acceptance. Correspondingly, the variable $\tilde{\xi}$ is defined as

$$\tilde{\xi} \simeq M_X^2/s = \sum p_T e^{\pm\eta}/\sqrt{s}. \quad (2)$$

At the detector level, the sum in Eq. (2) runs over calorimeter clusters in the region $|\eta| < 4.8$. To best match this requirement, the corrected cross section is defined in terms of neutral particles with $p > 200$ MeV and charged particles with $p > 500$ MeV in the same pseudorapidity range. The correlation at the particle level between $\tilde{\xi}$ and the true ξ (the latter obtained from elastically scattered protons) in the PYTHIA8 MC model of SD events with two jets, is shown in Fig. 2(a). For $\log_{10} \xi \lesssim -2$, there is a clear correlation between the fiducial $\tilde{\xi}$ variable and ξ , which continues to larger ξ , but with a progressively worse correspondence as some components of the dissociation system which are included in the ξ calculation fail the fiducial requirement $|\eta| < 4.8$ applied in the $\tilde{\xi}$ calculation. At low values, $\tilde{\xi}$ is systematically slightly smaller than ξ , due to the exclusion of low-momentum particles from the $\tilde{\xi}$ definition. Fig. 2(b) shows the correlation between the reconstructed and particle-level determinations of $\tilde{\xi}$. According to the MC models, the resolution in the absolute value of $\log_{10} \tilde{\xi}$ varies from around 0.07 at large $\tilde{\xi}$ values to around 0.14 at small $\tilde{\xi}$.

The quality of the description of the uncorrected data by the PYTHIA8 Monte Carlo model is shown for several variables in Fig. 3. Here, the default ND component of PYTHIA8 is fixed to match the data in the first bin of the $\Delta\eta^F$ distribution, requiring a normalisation factor of 0.71. The SD and DD contributions are shown without any adjustment of their normalisation. Satisfactory descriptions are obtained of the $\Delta\eta^F$ and $\tilde{\xi}$ variables, and also of the pseudorapidity and transverse momentum distributions of the leading jet, indicating that a combination of the diffractive and the non-diffractive PYTHIA8 components is appropriate for use in the unfolding of experimental effects.

The data distributions in $\Delta\eta^F$ and $\tilde{\xi}$ are corrected for detector acceptance and migrations between measurement bins due to finite experimental resolution using Iterative Dynamically Stabilised (IDS) unfolding [44]. This procedure corrects for migrations between the particle and detector levels based on an ‘unfolding’ matrix, constructed from a combination of PYTHIA8 ND, SD and DD samples, as shown in Fig. 2(b). The MC combination is optimised in a simple fitting procedure in which scaling factors are applied to the ND and (SD+DD) components to best match the data. The IDS unfolding is performed in two dimensions, corresponding to the p_T of the leading jet and the target distribution (either $\Delta\eta^F$ or $\tilde{\xi}$). The results of the IDS procedure depend in

general on the number of iterations used. A fast convergence is achieved for both measured distributions and the fourth iteration is chosen as nominal since it optimises the balance between the systematic and statistical uncertainty arising from the unfolding procedure. The unfolding procedure is stable against variations in binning, number of iterations and the scaling factors applied to the diffractive and non-diffractive contributions in the PYTHIA8 model, as discussed further in Section 5.

5. Systematic uncertainties

The procedures for handling many of the sources of systematic uncertainty follow from previous ATLAS measurements. The full list of uncertainties considered is given below. Further details of the uncertainties affecting jets (sources 1–5 below) can be found in Ref. [40], while those affecting diffractive variables (sources 7–9) are elaborated in Ref. [2,43].

1. **Jet energy scale:** the largest source of uncertainty arises from the determination of the jet energy scale. This is obtained following the procedure in Ref. [40], where relative shifts are applied between the particle-level and detector-level response as a function of η and p_T . This accounts for all effects playing a role in evaluating jet transverse momenta, including dead material, electronic noise, the different responses of the LAR and Tile calorimeters, the simulation of particle showers in the calorimeters, pile-up effects and the models of fragmentation used by different MC generators [45]. Studies in the context of the current analysis show that the inclusive treatment is also appropriate for diffractive processes. As in Ref. [40], the dominant component of this uncertainty comes from the inter-calibration of jets in η . The total resulting uncertainty in the differential cross sections measured here varies from 20% for small gaps to $\sim 40\%$ for very large gaps, a region which is dominated by diffractive events with relatively small transverse momentum or large pseudorapidity of jets.
2. **Jet energy resolution:** this is determined from data using in situ techniques and MC simulation [46]. The resulting uncertainty on the cross-section measurements is evaluated by smearing the p_T of the reconstructed jets in MC simulation using a Gaussian distribution to match the resolution uncertainty found in data. The resulting effect is below 6% in all kinematic regions.
3. **Jet angular resolution:** this was determined using the same techniques as for the jet energy resolution. Following the procedure in Ref. [40] leads to an uncertainty on the differential

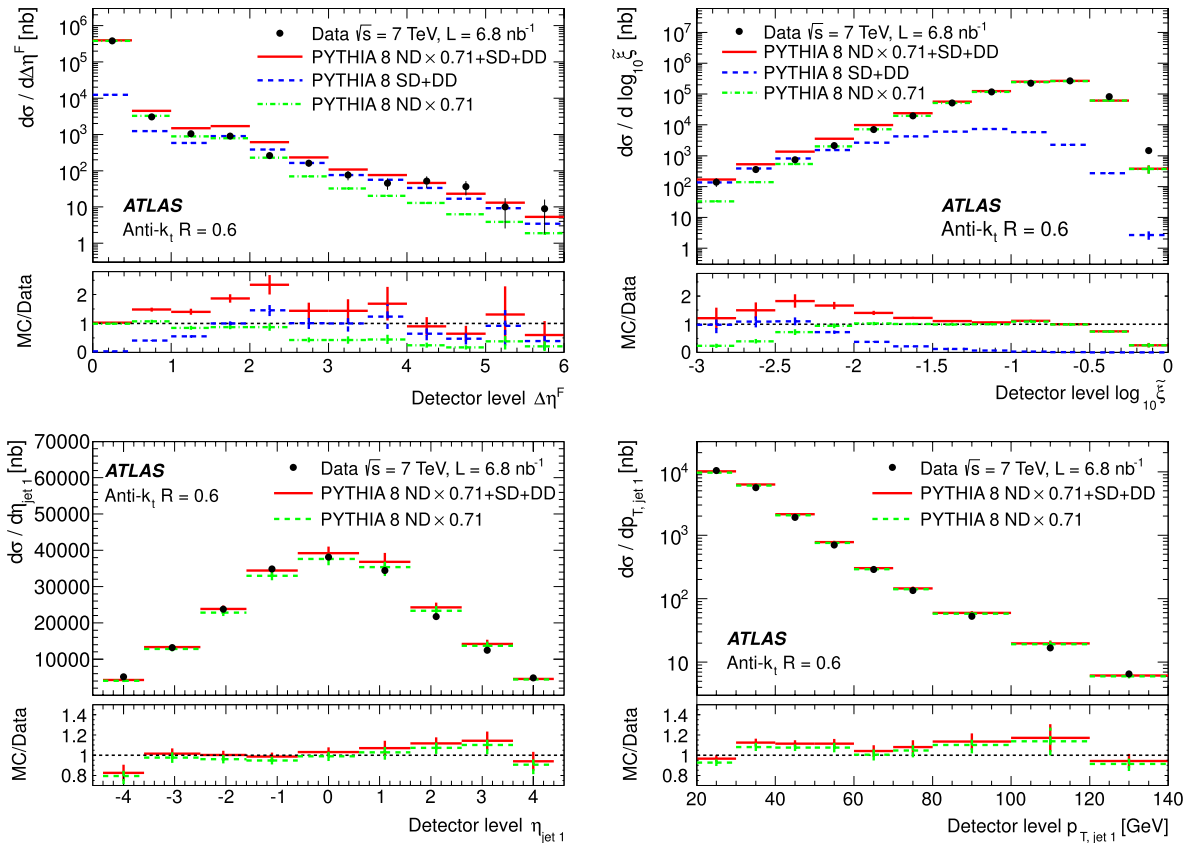


Fig. 3. Comparisons of dijet cross sections from uncorrected data with a combination of PYTHIA8 diffractive and non-diffractive contributions at detector level based on jets found by the anti- k_T algorithm with $R = 0.6$. The MC distributions are normalised to the integrated luminosity of the data after first applying a factor of 0.71 to the ND contribution. The error bars correspond to the statistical uncertainties. In addition to the measured (a) $\Delta\eta^F$ and (b) ξ variables, the distributions in (c) the leading-jet pseudorapidity and (d) transverse momentum are also shown. The lower panels show ratios of the MC models to the data where the error bars indicate the sum in quadrature of the statistical uncertainties arising from the data and the MC simulation.

cross sections which is typically around 1–2% and largest for jets at the largest $|\eta|$.

4. **Jet reconstruction efficiency:** the efficiency for reconstructing jets from the calorimeter information is determined by reference to a sample of ‘track jets’ reconstructed from inner-detector tracks. Following Ref. [40], the uncertainty is taken from the difference between the results of this procedure using data and MC simulation, with extrapolation to the η range not covered by the tracker. This results in systematic uncertainties in the measured cross sections which are smaller than 2% in all kinematic regions.
5. **Jet cleaning efficiency:** the fraction of jets that match the standard quality criteria, designed to remove jets associated with spurious calorimeter response, was studied using a tag-and-probe technique [40]. The corresponding systematic uncertainties are obtained by applying looser and tighter selections to the tag jet and propagate to at most 8% in the cross sections measured here.
6. **Trigger efficiency:** the trigger efficiency is evaluated as a function of leading-jet transverse momentum in various pseudorapidity ranges using either an independently triggered data sample or the MC mixture used in Fig. 3. The rise near the threshold of the efficiency in each p_T interval is parameterised based on a fit with free parameters. The efficiency is taken from the data, while the uncertainty is taken as the difference between two MC distributions: one assuming 100% trigger efficiency and the other rescaled by trigger efficiencies found in this MC sample in the same η and p_T ranges as in the data. The resulting uncertainties are smaller than 3.5% for all mea-

surements. A further parameterisation uncertainty, evaluated by varying the fit parameters within their uncertainties, is less than 0.7% for all measurements. An additional uncertainty, below 0.5% in all bins, is obtained from the differences in the simulated efficiencies from the ND, SD and DD processes.

7. **Cluster energy scale:** the uncertainty on the energy scale of the individual calorimeter clusters used to determine ξ is evaluated in an η -dependent manner as described in Ref. [43]. The resulting uncertainty in the cross sections differential in ξ is typically 10%.
8. **Cell significance threshold:** the significance thresholds applied to suppress calorimeter clusters which are consistent with noise fluctuations, are shifted up and down by 10% to determine the corresponding systematic uncertainties. The weakened requirements on particle (transverse) momenta applied here compared with Ref. [2] increase the sensitivity to the threshold shifts, particularly in the forward regions, resulting in uncertainties on the differential cross sections of typically 10–20%.
9. **Track reconstruction efficiency:** the uncertainty on the track reconstruction efficiency is taken from Ref. [42], resulting in a negligible effect on the differential cross sections.
10. **Luminosity:** the uncertainty on the luminosity is taken from the luminosity determination for the year 2010 [39], resulting in a $\pm 3.5\%$ normalisation uncertainty on all measurements.
11. **Reconstructed vertex requirement:** the uncertainty on the efficiency of the vertex multiplicity requirement is evaluated by loosening it in data to include events with no vertices. This

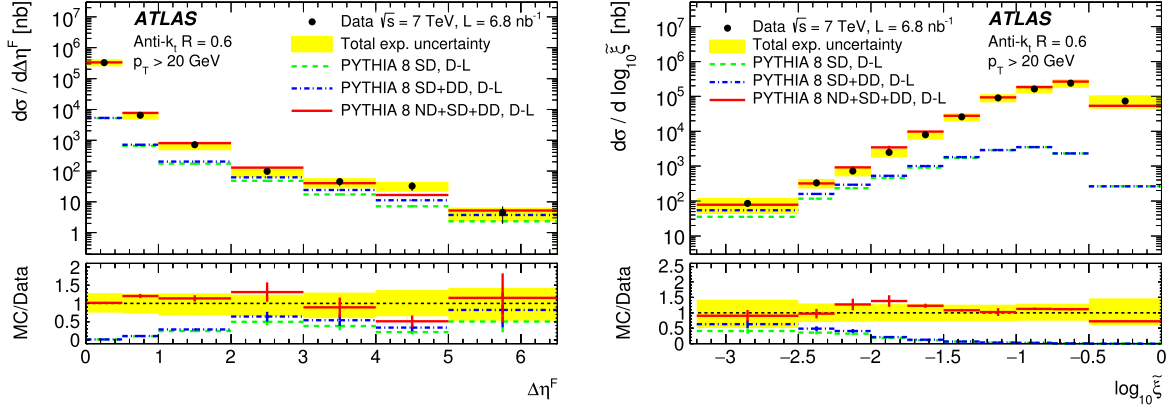


Fig. 4. The differential dijet cross sections in (a) $\Delta\eta^F$ and (b) $\tilde{\xi}$, compared with the particle-level PYTHIA8 model of the SD, sum of diffractive components SD and DD, and sum of all three ND, SD and DD components. The Donnachie–Landshoff pomeron flux model is used for the diffractive components. The error bars on the data and the MC models indicate their respective statistical uncertainties, while the yellow bands show the total uncertainties on the data. The ND contribution is normalised to match the data in the first $\Delta\eta^F$ bin. The lower panels show ratios of the MC models to the data where the error bars indicate the sum in quadrature of the statistical uncertainties arising from the data and the MC simulation. (For interpretation of the references to color in this figure legend, the reader is referred to the web version of this article.)

changes the differential cross sections by less than 1% in all bins.

12. **Dead material:** the effect of possible inaccuracies in the detector dead material simulation was studied in Ref. [2] using dedicated MC samples with modified material budgets ($\pm 10\%$ around the central value) in the inner detector, services and calorimeters. The largest effect on any bin in that analysis was 3%, which is applied as a symmetric shift in each bin of the current measurement.
13. **Unfolding procedure:** the uncertainty associated with modelling bias introduced by the unfolding procedure is estimated using a data-driven procedure whereby the particle-level distributions of the MC sample are reweighted such that the corresponding detector-level distributions match the uncorrected data in the two-dimensional $(\Delta\eta^F, \tilde{\xi})$ -space. The reweighted detector-level MC distribution is then unfolded using the same procedure as is applied to the data. The systematic uncertainty in each bin is taken to be the difference between the unfolded reweighted MC distribution and the reweighted particle-level MC distribution. The resulting unfolding uncertainty is typically around 15% for the $\Delta\eta^F$ distribution (rising to 25% in the bin for the largest gaps) and is smaller than 10% in the case of the $\tilde{\xi}$ distribution. Since the factors used to scale the ND and (SD+DD) processes to best describe the data before unfolding are different for the $\Delta\eta^F$ and $\tilde{\xi}$ distributions, a further uncertainty of up to around 5% is ascribed by swapping these factors between the two distributions.

The total systematic uncertainty is defined as the sum in quadrature of the uncertainties described above. The dominant contribution arises from the jet energy scale uncertainty, followed by the unfolding uncertainty, the cell significance threshold uncertainty (for the $\Delta\eta^F$ distribution) and the cluster energy scale uncertainty (for $\tilde{\xi}$). The overall uncertainty varies between bins in the range 20% to 45%. There are strong correlations between the systematic uncertainties in neighbouring measurement intervals of both the $\Delta\eta^F$ and $\tilde{\xi}$ distributions.

6. Results

In this section, particle-level dijet cross sections are presented differentially in the variables $\Delta\eta^F$ and $\tilde{\xi}$, both of which have discriminatory power to separate diffractive and non-diffractive contributions. The cross sections correspond to events with at least

two jets with $p_T > 20$ GeV in the region $|\eta| < 4.4$. The particle-level gap is defined by the region of pseudorapidity with an absence of neutral particles with $p > 200$ MeV and charged particles with either $p > 500$ MeV or $p_T > 200$ MeV. The conclusions are not strongly dependent on the choice of R parameter in the anti- k_t jet algorithm, although the cross-section normalisations are about two times larger for $R = 0.6$ than for $R = 0.4$. The data shown here correspond to $R = 0.6$. The results with both cone sizes can be found in tabular form in Ref. [47].

Figs. 4(a) and 4(b) show the dijet cross section differentially in $\Delta\eta^F$ and $\tilde{\xi}$ for $R = 0.6$ jets. In contrast to related distributions in inclusive rapidity-gap measurements [2], the data in these figures do not show any significant diffractive plateau at large gap sizes. This difference is of kinematic origin, resulting from the reduced phase space at large gap sizes or small $\tilde{\xi}$ when high- p_T jets are required. Both distributions are compared with predictions from the PYTHIA8 MC model, decomposed into ND, SD and DD components, with the D–L flux choice. The normalisation of the ND contribution in both distributions is fixed to match the data in the first bin of $\Delta\eta^F$, where this component is expected to be heavily dominant, requiring a multiplicative factor of 1/1.4. The SD and DD normalisations are left unchanged from their defaults in PYTHIA8. This MC combination results in a satisfactory description of both distributions. The ND component is at least an order of magnitude larger than the SD and DD contributions for relatively small $\Delta\eta^F \lesssim 1$ and large $\tilde{\xi} \gtrsim 0.1$. As $\Delta\eta^F$ grows or $\tilde{\xi}$ falls, the diffractive components of the models become increasingly important, such that the ND and (SD+DD) components are approximately equal at $\Delta\eta^F \sim 3$ or $\log_{10} \tilde{\xi} \sim -2$. At the largest gaps ($\Delta\eta^F \gtrsim 5$) and smallest $\tilde{\xi}$ ($\tilde{\xi} \lesssim 0.003$), the model suggests that the diffractive components are approximately twice as large as the ND contribution.

A dijet cross section differential in $\tilde{\xi}$ has also been measured by CMS [15]. The ATLAS and CMS hadron level cross-section definitions are slightly different in terms of the η , p and p_T ranges of the particles considered and the jet R parameter. Nonetheless, the measured cross sections are similar in magnitude and both analyses lead to the conclusion that a non-negligible ND contribution extends to relatively large $\Delta\eta^F$ and small $\tilde{\xi}$.

The predicted ND contribution at large gap sizes is sensitive to the modelling of rapidity and transverse momentum fluctuations in the hadronisation process, which are not yet well constrained. To establish the presence of a diffractive contribution, it is therefore necessary to investigate the likely range of ND predictions. In Fig. 5, the dijet cross sections differential in $\Delta\eta^F$ and $\tilde{\xi}$ are

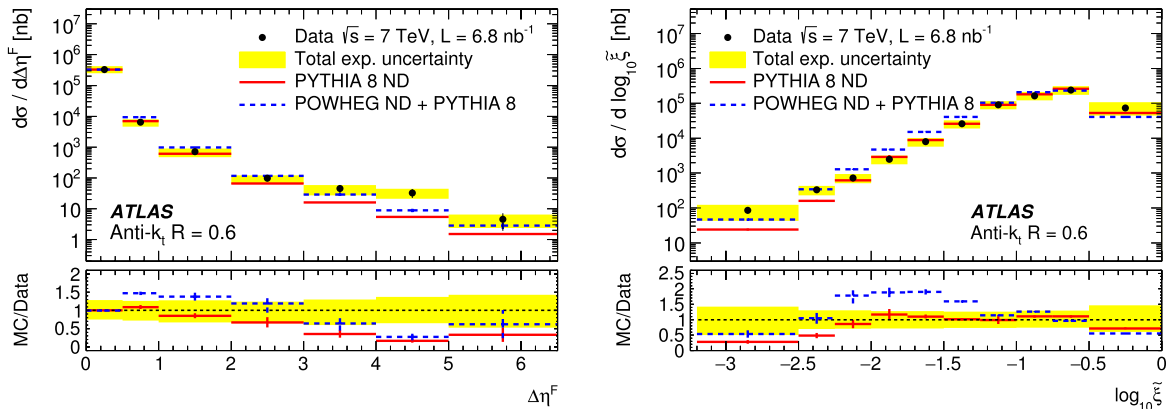


Fig. 5. The dijet cross sections differential in (a) $\Delta\eta^F$ and (b) $\xi_{\tilde{}}^F$, compared with the PYTHIA8 ND MC model as well as an ND model using the NLO POWHEG generator with hadronisation based on PYTHIA8. Each of the models is separately normalised to match the data in the first $\Delta\eta^F$ bin. The error bars on the data and the MC models indicate their respective statistical uncertainties, while the yellow bands show the total uncertainties on the data. The lower panels show ratios of the MC models to the data where the error bars indicate the sum in quadrature of the statistical uncertainties arising from the data and the MC simulation. (For interpretation of the references to color in this figure legend, the reader is referred to the web version of this article.)

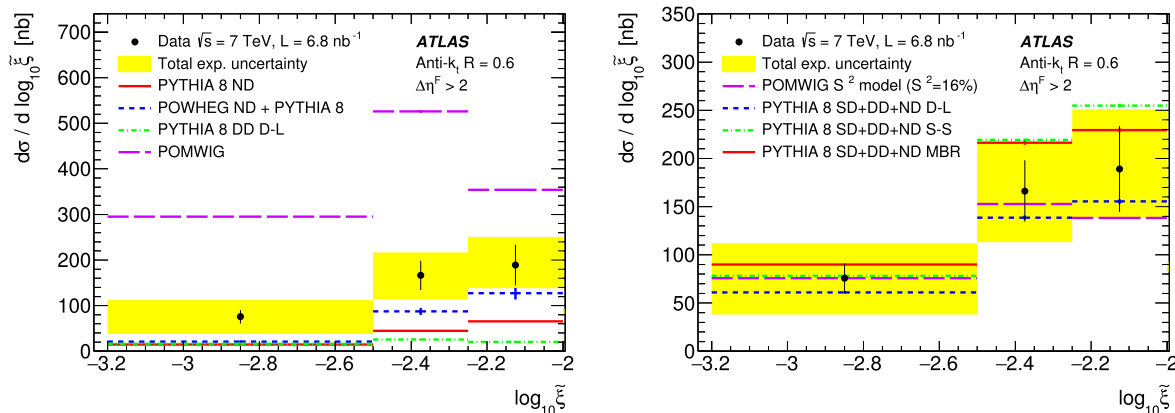


Fig. 6. The differential cross section as a function of $\xi_{\tilde{}}^F$ for events satisfying $\Delta\eta^F > 2$. The same data are shown in (a) and (b), and are compared with models as described in the text. The error bars on the data and the MC models indicate their respective statistical uncertainties, while the yellow bands show the total uncertainties on the data. The ‘POMWIG S^2 ’ model represents the sum of PYTHIA ND and POMWIG, with POMWIG multiplied by 0.16 and scaled by 1/1.23 and by the (SD+DD)/SD ratio from PYTHIA8. (For interpretation of the references to color in this figure legend, the reader is referred to the web version of this article.)

compared with the PYTHIA8 ND contribution and also with an NLO calculation of non-diffractive dijet production in the POWHEG framework, with hadronisation modelled using PYTHIA8, as described in Section 2. Each of the ND predictions is separately normalised in the first bin of the $\Delta\eta^F$ distribution. The range spanned by the ND predictions suggests a substantial uncertainty in the probability of producing gaps through hadronisation fluctuations, such that for $\Delta\eta^F \lesssim 4$, it is not possible to draw conclusions on the presence or absence of an additional diffractive contribution. However, in both of the models, the ND prediction falls significantly short of the data for $\Delta\eta^F \gtrsim 4$. A similar conclusion is reached at the lowest $\xi_{\tilde{}}^F$. This region is therefore investigated in more detail in the following.

Since the diffractive contribution is characterised by both large $\Delta\eta^F$ and small $\xi_{\tilde{}}^F$, it can be separated most cleanly by placing requirements on both variables simultaneously. In Fig. 6, the $\xi_{\tilde{}}^F$ distribution is shown after applying the requirement $\Delta\eta^F > 2$. This restricts the accessible kinematic range to $\xi_{\tilde{}}^F \lesssim 0.01$, and suppresses the ND contributions considerably. As shown in Fig. 6(a), the ND contribution in the lowest $\xi_{\tilde{}}^F$ bin ($-3.2 < \log_{10} \xi_{\tilde{}}^F < -2.5$) is smaller than 25% according to all models considered, allowing for a quantitative investigation of the diffractive contribution.

The data are compared with various models of diffractive dijet production with no rapidity-gap survival probability factors ap-

plied. The PYTHIA8 ND+SD+DD model is shown in Fig. 6(b) for three different choices of pomeron flux, Schuler–Sjöstrand (S–S), Donnachie–Landshoff (D–L) and Minimum Bias Rockefeller (MBR), as described in Section 2. The SD contribution dominates in this kinematic region, as can be inferred by comparing the PYTHIA8 predictions in Fig. 6(b) with the PYTHIA8 ND and PYTHIA8 DD contributions in Fig. 6(a). There is some dependence of the predicted cross section on the choice of flux, but all three PYTHIA8 predictions are compatible with the data without the need for a rapidity-gap survival probability factor, the D–L flux giving the best description. In contrast, the POMWIG model of the SD contribution alone lies above the data by around a factor of three in the low $\xi_{\tilde{}}^F$, large $\Delta\eta^F$ region (Fig. 6(a)).

Both PYTHIA8 and POMWIG are based on implementations of DPDFs as measured at HERA. POMWIG is a straightforward implementation of a standard factorisable Pomeron model with standard matrix elements, specifically intended for use in comparison with diffractive hard scattering processes such as that measured in this paper. PYTHIA8 is intended to describe diffraction inclusively. It contains a complex transition between the hard (DPDF-based) and soft models, and the corresponding mechanisms for generating final-state particles. The large difference here between the predictions of PYTHIA8 and POMWIG may be a consequence of this difference in basic approach. The quality of the description of

the data by PYTHIA8 is not altered significantly if the modelling of multi-particle interactions, colour reconnections, or initial- or final-state radiation are varied.

Attributing the POMWIG model's excess over the data in the most sensitive region to absorptive effects, the data are compared quantitatively with POMWIG to determine the rapidity-gap survival probability S^2 appropriate to this model. The value of S^2 is determined from the region where the poorly known ND contribution is smallest, i.e. integrated over the range $-3.2 < \log_{10} \tilde{\xi} < -2.5$ after imposing the rapidity-gap requirement $\Delta\eta^F > 2$ as in Fig. 6. The estimate of S^2 is obtained from the ratio of data to the SD contribution in the POMWIG model after subtracting from the data the ND contribution as modelled by PYTHIA8 and the DD contribution assuming the SD/(SD+DD) ratio from PYTHIA8. No gap survival factors are applied to the subtracted ND and DD contributions. The size of these corrections can be inferred from the PYTHIA8 ND and DD contributions as indicated in Fig. 6(a). A correction factor 1.23 ± 0.16 [48] is applied to S^2 to account for the fact that the H1 2006 Fit B DPDFs used in POMWIG include proton dissociation contributions $ep \rightarrow eXY$ where the proton excitation has a mass $M_Y < 1.6$ GeV, in addition to the SD process.

The resulting extracted value of the rapidity-gap survival probability appropriate to the mixed POMWIG/PYTHIA8 model is

$$S^2 = 0.16 \pm 0.04 (\text{stat.}) \pm 0.08 (\text{exp. syst.}),$$

where the statistical (stat.) and experimental systematic (exp. syst.) uncertainties are propagated from the data. This model is shown as 'POMWIG S^2 Model' in Fig. 6(b). No attempt has been made to fully assess the model-dependence uncertainty, although changing the ND contribution in the extraction from PYTHIA8 to POWHEG + PYTHIA8 results in an S^2 of 0.15 and indications from elsewhere [14,15] suggest that S^2 might be smaller if NLO models were used. The result is compatible with the values of 0.12 ± 0.05 and 0.08 ± 0.04 , obtained by CMS in LO and NLO analyses, respectively, using the region $0.0003 < \tilde{\xi} < 0.002$ and a jet R parameter of 0.5 [15]. The result is also compatible with that obtained at lower centre-of-mass energy at the Tevatron [7], which was re-evaluated in a subsequent NLO analysis [49] to be between 0.05 and 0.3, depending on the fraction of the pomeron momentum carried by the parton entering the hard scattering. Theoretical predictions for S^2 at the LHC [50,51] are also compatible with the result here, although the predicted decrease with increasing centre-of-mass energy is not yet established.

7. Conclusions

An ATLAS measurement of the cross section for dijet production in association with forward rapidity gaps is reported, based on 6.8 nb^{-1} low pile-up 7 TeV pp collision data taken at the LHC in 2010. The data are characterised according to the size of the forward rapidity gap, quantified by $\Delta\eta^F$ and $\tilde{\xi}$, which for the single-diffractive case approximates the fractional longitudinal momentum loss of the scattered proton using the information available within the detector acceptance. Non-diffractive Monte Carlo models are capable of describing the data over a wide kinematic range. However, a diffractive component is also required for a more complete description of the data, particularly when both large $\Delta\eta^F$ and small $\tilde{\xi}$ are required. The PYTHIA8 model gives the best description of the shape and normalisation of this contribution.

The rapidity-gap survival probability is estimated by comparing the measured cross section for events with both large $\Delta\eta^F$ and small $\tilde{\xi}$ with the leading-order POMWIG Monte Carlo model of the diffractive contribution, derived from diffractive parton distribution functions extracted in deep inelastic ep scattering. This determi-

nation is limited by the uncertainties associated with the non-diffractive and double-dissociation contributions, the result being $S^2 = 0.16 \pm 0.04$ (stat.) ± 0.08 (exp. syst.).

Acknowledgements

We thank CERN for the very successful operation of the LHC, as well as the support staff from our institutions without whom ATLAS could not be operated efficiently.

We acknowledge the support of ANPCyT, Argentina; YerPhI, Armenia; ARC, Australia; BMWFW and FWF, Austria; ANAS, Azerbaijan; SSTC, Belarus; CNPq and FAPESP, Brazil; NSERC, NRC and CFI, Canada; CERN; CONICYT, Chile; CAS, MOST and NSFC, China; COLCIENCIAS, Colombia; MSMT CR, MPO CR and VSC CR, Czech Republic; DNRF, DNSRC and Lundbeck Foundation, Denmark; IN2P3-CNRS, CEA-DSM/IRFU, France; GNSF, Georgia; BMBF, HGF, and MPG, Germany; GSRT, Greece; RGC, Hong Kong SAR, China; ISF, I-CORE and Benoziyo Center, Israel; INFN, Italy; MEXT and JSPS, Japan; CNRST, Morocco; FOM and NWO, Netherlands; RCN, Norway; MNiSW and NCN, Poland; FCT, Portugal; MNE/IFA, Romania; MES of Russia and NRC KI, Russian Federation; JINR; MESTD, Serbia; MSSR, Slovakia; ARRS and MIZŠ, Slovenia; DST/NRF, South Africa; MINECO, Spain; SRC and Wallenberg Foundation, Sweden; SERI, SNSF and Cantons of Bern and Geneva, Switzerland; MOST, Taiwan; TAEK, Turkey; STFC, United Kingdom; DOE and NSF, United States of America. In addition, individual groups and members have received support from BCKDF, the Canada Council, CANARIE, CRC, Compute Canada, FQRNT, and the Ontario Innovation Trust, Canada; EPLANET, ERC, FP7, Horizon 2020 and Marie Skłodowska-Curie Actions, European Union; Investissements d'Avenir Labex and IDEX, ANR, Region Auvergne and Fondation Partager le Savoir, France; DFG and AvH Foundation, Germany; Herakleitos, Thales and Aristeia programmes co-financed by EU-ESF and the Greek NSRF; BSF, GIF and Minerva, Israel; BRF, Norway; the Royal Society and Leverhulme Trust, United Kingdom.

The crucial computing support from all WLCG partners is acknowledged gratefully, in particular from CERN and the ATLAS Tier-1 facilities at TRIUMF (Canada), NDGF (Denmark, Norway, Sweden), CC-IN2P3 (France), KIT/GridKA (Germany), INFN-CNAF (Italy), NL-T1 (Netherlands), PIC (Spain), ASGC (Taiwan), RAL (UK) and BNL (USA) and in the Tier-2 facilities worldwide.

References

- [1] ATLAS Collaboration, Measurement of the inelastic proton–proton cross-section at $\sqrt{s} = 7$ TeV with the ATLAS detector, Nat. Commun. 2 (2011) 463, arXiv:1104.0326 [hep-ex].
- [2] ATLAS Collaboration, Rapidity gap cross sections measured with the ATLAS detector in pp collisions at $\sqrt{s} = 7$ TeV, Eur. Phys. J. C 72 (2012) 1926, arXiv:1201.2808 [hep-ex].
- [3] CMS Collaboration, Measurement of diffraction dissociation cross sections in pp collisions at $\sqrt{s} = 7$ TeV, Phys. Rev. D 92 (2015) 012003, arXiv:1503.08689 [hep-ex].
- [4] R. Bonino, et al., UA8 Collaboration, Evidence for transverse jets in high mass diffraction, Phys. Lett. B 211 (1988) 239.
- [5] C. Adloff, et al., H1 Collaboration, Diffractive jet production in deep inelastic e^+p collisions at HERA, Eur. Phys. J. C 20 (2001) 29–49, arXiv:hep-ex/0012051 [hep-ex].
- [6] F.D. Aaron, et al., H1 Collaboration, Diffractive dijet photoproduction in ep collisions at HERA, Eur. Phys. J. C 70 (2010) 15–37, arXiv:1006.0946 [hep-ex].
- [7] T. Affolder, et al., CDF Collaboration, Diffractive dijets with a leading antiproton in $\bar{p}p$ collisions at $\sqrt{s} = 1800$ GeV, Phys. Rev. Lett. 84 (2000) 5043–5048.
- [8] G. Ingelman, P. Schlein, Jet structure in high mass diffractive scattering, Phys. Lett. B 152 (1985) 256.
- [9] E. Feinberg, I. Pomeranchuk, High-energy inelastic diffraction phenomena, Suppl. Nuovo Cim. 3 (1956) 652.
- [10] P. Newman, M. Wing, The hadronic final state at HERA, Rev. Mod. Phys. 86 (2014) 1037, arXiv:1308.3368 [hep-ex].

- [11] A. Aktas, et al., H1 Collaboration, Measurement and QCD analysis of the diffractive deep-inelastic scattering cross-section at HERA, *Eur. Phys. J. C* 48 (2006) 715–748, arXiv:hep-ex/0606004 [hep-ex].
- [12] S. Chekanov, et al., ZEUS Collaboration, A QCD analysis of ZEUS diffractive data, *Nucl. Phys. B* 831 (2010) 1–25, arXiv:0911.4119 [hep-ex].
- [13] A. Aktas, et al., H1 Collaboration, Tests of QCD factorisation in the diffractive production of dijets in deep-inelastic scattering and photoproduction at HERA, *Eur. Phys. J. C* 51 (2007) 549–568, arXiv:hep-ex/0703022 [hep-ex].
- [14] V. Andreev, et al., Diffractive dijet production with a leading proton in *ep* collisions at HERA, *J. High Energy Phys.* 05 (2015) 056, arXiv:1502.01683 [hep-ex].
- [15] CMS Collaboration, Observation of a diffractive contribution to dijet production in proton–proton collisions at $\sqrt{s} = 7$ TeV, *Phys. Rev. D* 87 (2013) 012006, arXiv:1209.1805 [hep-ex].
- [16] ATLAS Collaboration, Measurement of underlying event characteristics using charged particles in *pp* collisions at $\sqrt{s} = 900$ GeV and 7 TeV with the ATLAS detector, *Phys. Rev. D* 83 (2011) 112001, arXiv:1012.0791 [hep-ex].
- [17] ATLAS Collaboration, Measurement of the underlying event in jet events from 7 TeV proton–proton collisions with the ATLAS detector, *Eur. Phys. J. C* 74 (2014) 2965, arXiv:1406.0392 [hep-ex].
- [18] ATLAS Collaboration, Measurement of distributions sensitive to the underlying event in inclusive Z-boson production in *pp* collisions at $\sqrt{s} = 7$ TeV with the ATLAS detector, *Eur. Phys. J. C* 74 (2014) 3195, arXiv:1409.3433 [hep-ex].
- [19] T. Sjöstrand, S. Mrenna, P.Z. Skands, A brief introduction to PYTHIA 8.1, *Comput. Phys. Commun.* 178 (2008) 852–867, arXiv:0710.3820 [hep-ph].
- [20] B.E. Cox, J.R. Forshaw, POMWIG: HERWIG for diffractive interactions, *Comput. Phys. Commun.* 144 (2002) 104–110, arXiv:hep-ph/0010303 [hep-ph].
- [21] P. Nason, A new method for combining NLO QCD with shower Monte Carlo algorithms, *J. High Energy Phys.* 0411 (2004) 040, arXiv:hep-ph/0409146 [hep-ph].
- [22] S. Alioli, et al., Jet pair production in POWHEG, *J. High Energy Phys.* 1104 (2011) 081, arXiv:1012.3380 [hep-ph].
- [23] D. Stump, et al., Inclusive jet production, parton distributions, and the search for new physics, *J. High Energy Phys.* 0310 (2003) 046, arXiv:hep-ph/0303013.
- [24] S. Navin, Diffraction in Pythia, arXiv:1005.3894 [hep-ph], 2010.
- [25] T. Sjöstrand, S. Mrenna, P.Z. Skands, PYTHIA 6.4 physics and manual, *J. High Energy Phys.* 0605 (2006) 026, arXiv:hep-ph/0603175 [hep-ph].
- [26] H.-L. Lai, et al., New parton distributions for collider physics, *Phys. Rev. D* 82 (2010) 074024, arXiv:1007.2241 [hep-ph].
- [27] G.A. Schuler, T. Sjöstrand, Hadronic diffractive cross-sections and the rise of the total cross-section, *Phys. Rev. D* 49 (1994) 2257–2267.
- [28] A. Donnachie, P. Landshoff, Elastic scattering and diffraction dissociation, *Nucl. Phys. B* 244 (1984) 322.
- [29] E.L. Berger, et al., Diffractive hard scattering, *Nucl. Phys. B* 286 (1987) 704.
- [30] K. Streng, Hard QCD scatterings in diffractive reactions at HERA, CERN-TH-4949, 1988.
- [31] R. Ciesielski, K. Goulianos, MBR Monte Carlo simulation in PYTHIA8, *PoS ICHHEP2012* (2013) 301, arXiv:1205.1446 [hep-ph].
- [32] B. Andersson, et al., Parton fragmentation and string dynamics, *Phys. Rep.* 97 (1983) 31–145.
- [33] G. Marchesini, et al., HERWIG: a Monte Carlo event generator for simulating hadron emission reactions with interfering gluons. Version 5.1 – April 1991, *Comput. Phys. Commun.* 67 (1992) 465–508.
- [34] ATLAS Collaboration, Summary of ATLAS Pythia 8 tunes, ATL-PHYS-PUB-2012-003, <http://cds.cern.ch/record/1474107>, 2012.
- [35] S. Agostinelli, et al., GEANT4: a simulation toolkit, *Nucl. Instrum. Methods A* 506 (2003) 250.
- [36] ATLAS Collaboration, The ATLAS simulation infrastructure, *Eur. Phys. J. C* 70 (2010) 823, arXiv:1005.4568 [hep-ex].
- [37] ATLAS Collaboration, The ATLAS experiment at the CERN large hadron collider, *J. Instrum.* 3 (2008) S08003.
- [38] ATLAS Collaboration, Luminosity determination in *pp* collisions at $\sqrt{s} = 7$ TeV using the ATLAS detector at the LHC, *Eur. Phys. J. C* 71 (2011) 1630, arXiv:1101.2185 [hep-ex].
- [39] ATLAS Collaboration, Improved luminosity determination in *pp* collisions at $\sqrt{s} = 7$ TeV using the ATLAS detector at the LHC, *Eur. Phys. J. C* 73 (2013) 2518, arXiv:1302.4393 [hep-ex].
- [40] ATLAS Collaboration, Measurement of inclusive jet and dijet production in *pp* collisions at $\sqrt{s} = 7$ TeV using the ATLAS detector, *Phys. Rev. D* 86 (2012) 014022, arXiv:1112.6297 [hep-ex].
- [41] M. Cacciari, G.P. Salam, G. Soyez, The anti- $k(t)$ jet clustering algorithm, *J. High Energy Phys.* 0804 (2008) 063, arXiv:0802.1189 [hep-ph].
- [42] ATLAS Collaboration, Charged-particle multiplicities in *pp* interactions measured with the ATLAS detector at the LHC, *New J. Phys.* 13 (2011) 053033, arXiv:1012.5104 [hep-ex].
- [43] ATLAS Collaboration, Measurements of the pseudorapidity dependence of the total transverse energy in proton–proton collisions at $\sqrt{s} = 7$ TeV with ATLAS, *J. High Energy Phys.* 1211 (2012) 033, arXiv:1208.6256 [hep-ex].
- [44] B. Malaescu, An iterative, dynamically stabilized (IDS) method of data unfolding, arXiv:1106.3107 [physics.data-an], 2011.
- [45] ATLAS Collaboration, Jet energy measurement and its systematic uncertainty in proton–proton collisions at $\sqrt{s} = 7$ TeV with the ATLAS detector, *Eur. Phys. J. C* 75 (2015) 17, arXiv:1406.0076 [hep-ex].
- [46] ATLAS Collaboration, Jet energy resolution in proton–proton collisions at $\sqrt{s} = 7$ TeV recorded in 2010 with the ATLAS detector, *Eur. Phys. J. C* 73 (2013) 2306, arXiv:1210.6210 [hep-ex].
- [47] HepData, 2015, hepdata.cedar.ac.uk.
- [48] A. Aktas, et al., H1 Collaboration, Diffractive deep-inelastic scattering with a leading proton at HERA, *Eur. Phys. J. C* 48 (2006) 749–766, arXiv:hep-ex/0606003 [hep-ex].
- [49] M. Klasen, G. Kramer, Survival probability for diffractive dijet production in *p* anti-*p* collisions from next-to-leading order calculations, *Phys. Rev. D* 80 (2009) 074006, arXiv:0908.2531 [hep-ph].
- [50] A. Kaidalov, et al., Factorization breaking in diffractive dijet production, *Phys. Lett. B* 559 (2003) 235–238, arXiv:hep-ph/0302091 [hep-ph].
- [51] V.A. Khoze, A.D. Martin, M. Ryskin, Soft diffraction and the elastic slope at Tevatron and LHC energies: a MultiPomeron approach, *Eur. Phys. J. C* 18 (2000) 167–179, arXiv:hep-ph/0007359 [hep-ph].

ATLAS Collaboration

G. Aad⁸⁵, B. Abbott¹¹³, J. Abdallah¹⁵¹, O. Abidinov¹¹, R. Aben¹⁰⁷, M. Abolins⁹⁰, O.S. AbouZeid¹⁵⁸, H. Abramowicz¹⁵³, H. Abreu¹⁵², R. Abreu¹¹⁶, Y. Abulaiti^{146a,146b}, B.S. Acharya^{164a,164b,a}, L. Adamczyk^{38a}, D.L. Adams²⁵, J. Adelman¹⁰⁸, S. Adomeit¹⁰⁰, T. Adye¹³¹, A.A. Affolder⁷⁴, T. Agatonovic-Jovin¹³, J. Agricola⁵⁴, J.A. Aguilar-Saavedra^{126a,126f}, S.P. Ahlen²², F. Ahmadov^{65,b}, G. Aielli^{133a,133b}, H. Akerstedt^{146a,146b}, T.P.A. Åkesson⁸¹, A.V. Akimov⁹⁶, G.L. Alberghi^{20a,20b}, J. Albert¹⁶⁹, S. Albrand⁵⁵, M.J. Alconada Verzini⁷¹, M. Aleksa³⁰, I.N. Aleksandrov⁶⁵, C. Alexa^{26b}, G. Alexander¹⁵³, T. Alexopoulos¹⁰, M. Alhroob¹¹³, G. Alimonti^{91a}, L. Alio⁸⁵, J. Alison³¹, S.P. Alkire³⁵, B.M.M. Allbrooke¹⁴⁹, P.P. Allport¹⁸, A. Aloisio^{104a,104b}, A. Alonso³⁶, F. Alonso⁷¹, C. Alpigiani¹³⁸, A. Altheimer³⁵, B. Alvarez Gonzalez³⁰, D. Álvarez Piqueras¹⁶⁷, M.G. Alviggi^{104a,104b}, B.T. Amadio¹⁵, K. Amako⁶⁶, Y. Amaral Coutinho^{24a}, C. Amelung²³, D. Amidei⁸⁹, S.P. Amor Dos Santos^{126a,126c}, A. Amorim^{126a,126b}, S. Amoroso⁴⁸, N. Amram¹⁵³, G. Amundsen²³, C. Anastopoulos¹³⁹, L.S. Ancu⁴⁹, N. Andari¹⁰⁸, T. Andeen³⁵, C.F. Anders^{58b}, G. Anders³⁰, J.K. Anders⁷⁴, K.J. Anderson³¹, A. Andreazza^{91a,91b}, V. Andrei^{58a}, S. Angelidakis⁹, I. Angelozzi¹⁰⁷, P. Anger⁴⁴, A. Angerami³⁵, F. Anghinolfi³⁰, A.V. Anisenkov^{109,c}, N. Anjos¹², A. Annovi^{124a,124b}, M. Antonelli⁴⁷, A. Antonov⁹⁸, J. Antos^{144b}, F. Anulli^{132a}, M. Aoki⁶⁶, L. Aperio Bella¹⁸, G. Arabidze⁹⁰, Y. Arai⁶⁶, J.P. Araque^{126a}, A.T.H. Arce⁴⁵, F.A. Arduh⁷¹, J-F. Arguin⁹⁵, S. Argyropoulos⁶³, M. Arik^{19a}, A.J. Armbruster³⁰, O. Arnaez³⁰, H. Arnold⁴⁸, M. Arratia²⁸, O. Arslan²¹, A. Artamonov⁹⁷, G. Artoni²³, S. Asai¹⁵⁵, N. Asbah⁴², A. Ashkenazi¹⁵³, B. Åsman^{146a,146b}, L. Asquith¹⁴⁹, K. Assamagan²⁵, R. Astalos^{144a}, M. Atkinson¹⁶⁵,

N.B. Atlay¹⁴¹, K. Augsten¹²⁸, M. Aourousseau^{145b}, G. Avolio³⁰, B. Axen¹⁵, M.K. Ayoub¹¹⁷, G. Azuelos^{95,d}, M.A. Baak³⁰, A.E. Baas^{58a}, M.J. Baca¹⁸, C. Bacci^{134a,134b}, H. Bachacou¹³⁶, K. Bachas¹⁵⁴, M. Backes³⁰, M. Backhaus³⁰, P. Bagiachi^{132a,132b}, P. Bagnaia^{132a,132b}, Y. Bai^{33a}, T. Bain³⁵, J.T. Baines¹³¹, O.K. Baker¹⁷⁶, E.M. Baldin^{109,c}, P. Balek¹²⁹, T. Balestri¹⁴⁸, F. Balli⁸⁴, W.K. Balunas¹²², E. Banas³⁹, Sw. Banerjee¹⁷³, A.A.E. Bannoura¹⁷⁵, L. Barak³⁰, E.L. Barberio⁸⁸, D. Barberis^{50a,50b}, M. Barbero⁸⁵, T. Barillari¹⁰¹, M. Barisonzi^{164a,164b}, T. Barklow¹⁴³, N. Barlow²⁸, S.L. Barnes⁸⁴, B.M. Barnett¹³¹, R.M. Barnett¹⁵, Z. Barnovska⁵, A. Baroncelli^{134a}, G. Barone²³, A.J. Barr¹²⁰, F. Barreiro⁸², J. Barreiro Guimarães da Costa⁵⁷, R. Bartoldus¹⁴³, A.E. Barton⁷², P. Bartos^{144a}, A. Basalaeu¹²³, A. Bassalat¹¹⁷, A. Basye¹⁶⁵, R.L. Bates⁵³, S.J. Batista¹⁵⁸, J.R. Batley²⁸, M. Battaglia¹³⁷, M. Baucé^{132a,132b}, F. Bauer¹³⁶, H.S. Bawa^{143,e}, J.B. Beacham¹¹¹, M.D. Beattie⁷², T. Beau⁸⁰, P.H. Beauchemin¹⁶¹, R. Beccherle^{124a,124b}, P. Bechtel²¹, H.P. Beck^{17,f}, K. Becker¹²⁰, M. Becker⁸³, M. Beckingham¹⁷⁰, C. Becot¹¹⁷, A.J. Beddall^{19b}, A. Beddall^{19b}, V.A. Bednyakov⁶⁵, C.P. Bee¹⁴⁸, L.J. Beemster¹⁰⁷, T.A. Beermann³⁰, M. Begel²⁵, J.K. Behr¹²⁰, C. Belanger-Champagne⁸⁷, W.H. Bell⁴⁹, G. Bella¹⁵³, L. Bellagamba^{20a}, A. Bellerive²⁹, M. Bellomo⁸⁶, K. Belotskiy⁹⁸, O. Beltramello³⁰, O. Benary¹⁵³, D. Benchechroun^{135a}, M. Bender¹⁰⁰, K. Bendtz^{146a,146b}, N. Benekos¹⁰, Y. Benhammou¹⁵³, E. Benhar Noccioli⁴⁹, J.A. Benitez Garcia^{159b}, D.P. Benjamin⁴⁵, J.R. Bensinger²³, S. Bentvelsen¹⁰⁷, L. Beresford¹²⁰, M. Beretta⁴⁷, D. Berge¹⁰⁷, E. Bergeaas Kuutmann¹⁶⁶, N. Berger⁵, F. Berghaus¹⁶⁹, J. Beringer¹⁵, C. Bernard²², N.R. Bernard⁸⁶, C. Bernius¹¹⁰, F.U. Bernlochner²¹, T. Berry⁷⁷, P. Berta¹²⁹, C. Bertella⁸³, G. Bertoli^{146a,146b}, F. Bertolucci^{124a,124b}, C. Bertsche¹¹³, D. Bertsche¹¹³, M.I. Besana^{91a}, G.J. Besjes³⁶, O. Bessidskaia Bylund^{146a,146b}, M. Bessner⁴², N. Besson¹³⁶, C. Betancourt⁴⁸, S. Bethke¹⁰¹, A.J. Bevan⁷⁶, W. Bhimji¹⁵, R.M. Bianchi¹²⁵, L. Bianchini²³, M. Bianco³⁰, O. Biebel¹⁰⁰, D. Biedermann¹⁶, S.P. Bieniek⁷⁸, N.V. Biesuz^{124a,124b}, M. Biglietti^{134a}, J. Bilbao De Mendizabal⁴⁹, H. Bilokon⁴⁷, M. Bindi⁵⁴, S. Binet¹¹⁷, A. Bingul^{19b}, C. Bini^{132a,132b}, S. Biondi^{20a,20b}, D.M. Bjergaard⁴⁵, C.W. Black¹⁵⁰, J.E. Black¹⁴³, K.M. Black²², D. Blackburn¹³⁸, R.E. Blair⁶, J.-B. Blanchard¹³⁶, J.E. Blanco⁷⁷, T. Blazek^{144a}, I. Bloch⁴², C. Blocker²³, W. Blum^{83,*}, U. Blumenschein⁵⁴, S. Blunier^{32a}, G.J. Bobbink¹⁰⁷, V.S. Bobrovnikov^{109,c}, S.S. Bocchetta⁸¹, A. Bocci⁴⁵, C. Bock¹⁰⁰, M. Boehler⁴⁸, J.A. Bogaerts³⁰, D. Bogavac¹³, A.G. Bogdanchikov¹⁰⁹, C. Bohm^{146a}, V. Boisvert⁷⁷, T. Bold^{38a}, V. Boldea^{26b}, A.S. Boldyrev⁹⁹, M. Bomben⁸⁰, M. Bona⁷⁶, M. Boonekamp¹³⁶, A. Borisov¹³⁰, G. Borissov⁷², S. Borroni⁴², J. Bortfeldt¹⁰⁰, V. Bortolotto^{60a,60b,60c}, K. Bos¹⁰⁷, D. Boscherini^{20a}, M. Bosman¹², J. Boudreau¹²⁵, J. Bouffard², E.V. Bouhova-Thacker⁷², D. Boumediene³⁴, C. Bourdarios¹¹⁷, N. Bousson¹¹⁴, S.K. Boutle⁵³, A. Boveia³⁰, J. Boyd³⁰, I.R. Boyko⁶⁵, I. Bozic¹³, J. Bracinik¹⁸, A. Brandt⁸, G. Brandt⁵⁴, O. Brandt^{58a}, U. Bratzler¹⁵⁶, B. Brau⁸⁶, J.E. Brau¹¹⁶, H.M. Braun^{175,*}, W.D. Breaden Madden⁵³, K. Brendlinger¹²², A.J. Brennan⁸⁸, L. Brenner¹⁰⁷, R. Brenner¹⁶⁶, S. Bressler¹⁷², T.M. Bristow⁴⁶, D. Britton⁵³, D. Britzger⁴², F.M. Brochu²⁸, I. Brock²¹, R. Brock⁹⁰, J. Bronner¹⁰¹, G. Brooijmans³⁵, T. Brooks⁷⁷, W.K. Brooks^{32b}, J. Brosamer¹⁵, E. Brost¹¹⁶, P.A. Bruckman de Renstrom³⁹, D. Bruncko^{144b}, R. Bruneliere⁴⁸, A. Bruni^{20a}, G. Bruni^{20a}, M. Bruschi^{20a}, N. Brusino²¹, L. Bryngemark⁸¹, T. Buanes¹⁴, Q. Buat¹⁴², P. Buchholz¹⁴¹, A.G. Buckley⁵³, S.I. Buda^{26b}, I.A. Budagov⁶⁵, F. Buehrer⁴⁸, L. Bugge¹¹⁹, M.K. Bugge¹¹⁹, O. Bulekov⁹⁸, D. Bullock⁸, H. Burckhart³⁰, S. Burdin⁷⁴, C.D. Burgard⁴⁸, B. Burghgrave¹⁰⁸, S. Burke¹³¹, I. Burmeister⁴³, E. Busato³⁴, D. Büscher⁴⁸, V. Büscher⁸³, P. Bussey⁵³, J.M. Butler²², A.I. Butt³, C.M. Buttar⁵³, J.M. Butterworth⁷⁸, P. Butti¹⁰⁷, W. Buttinger²⁵, A. Buzatu⁵³, A.R. Buzykaev^{109,c}, S. Cabrera Urbán¹⁶⁷, D. Caforio¹²⁸, V.M. Cairo^{37a,37b}, O. Cakir^{4a}, N. Calace⁴⁹, P. Calafiura¹⁵, A. Calandri¹³⁶, G. Calderini⁸⁰, P. Calfayan¹⁰⁰, L.P. Caloba^{24a}, D. Calvet³⁴, S. Calvet³⁴, R. Camacho Toro³¹, S. Camarda⁴², P. Camarri^{133a,133b}, D. Cameron¹¹⁹, R. Caminal Armadans¹⁶⁵, S. Campana³⁰, M. Campanelli⁷⁸, A. Campoverde¹⁴⁸, V. Canale^{104a,104b}, A. Canepa^{159a}, M. Cano Bret^{33e}, J. Cantero⁸², R. Cantrill^{126a}, T. Cao⁴⁰, M.D.M. Capeans Garrido³⁰, I. Caprini^{26b}, M. Caprini^{26b}, M. Capua^{37a,37b}, R. Caputo⁸³, R.M. Carbone³⁵, R. Cardarelli^{133a}, F. Cardillo⁴⁸, T. Carli³⁰, G. Carlino^{104a}, L. Carminati^{91a,91b}, S. Caron¹⁰⁶, E. Carquin^{32a}, G.D. Carrillo-Montoya³⁰, J.R. Carter²⁸, J. Carvalho^{126a,126c}, D. Casadei⁷⁸, M.P. Casado¹², M. Casolino¹², E. Castaneda-Miranda^{145a}, A. Castelli¹⁰⁷, V. Castillo Gimenez¹⁶⁷, N.F. Castro^{126a,g}, P. Catastini⁵⁷, A. Catinaccio³⁰, J.R. Catmore¹¹⁹, A. Cattai³⁰, J. Caudron⁸³, V. Cavaliere¹⁶⁵, D. Cavalli^{91a}, M. Cavalli-Sforza¹², V. Cavasinni^{124a,124b}, F. Ceradini^{134a,134b}, B.C. Cerio⁴⁵, K. Cerny¹²⁹, A.S. Cerqueira^{24b}, A. Cerri¹⁴⁹, L. Cerrito⁷⁶, F. Cerutti¹⁵, M. Cerv³⁰, A. Cervelli¹⁷, S.A. Cetin^{19c}, A. Chafaq^{135a}, D. Chakraborty¹⁰⁸, I. Chalupkova¹²⁹, Y.L. Chan^{60a}, P. Chang¹⁶⁵, J.D. Chapman²⁸,

D.G. Charlton¹⁸, C.C. Chau¹⁵⁸, C.A. Chavez Barajas¹⁴⁹, S. Cheatham¹⁵², A. Chegwidden⁹⁰, S. Chekanov⁶,
 S.V. Chekulaev^{159a}, G.A. Chelkov^{65,h}, M.A. Chelstowska⁸⁹, C. Chen⁶⁴, H. Chen²⁵, K. Chen¹⁴⁸,
 L. Chen^{33d,i}, S. Chen^{33c}, S. Chen¹⁵⁵, X. Chen^{33f}, Y. Chen⁶⁷, H.C. Cheng⁸⁹, Y. Cheng³¹, A. Cheplakov⁶⁵,
 E. Cheremushkina¹³⁰, R. Cherkaoui El Moursli^{135e}, V. Chernyatin^{25,*}, E. Cheu⁷, L. Chevalier¹³⁶,
 V. Chiarella⁴⁷, G. Chiarelli^{124a,124b}, G. Chiodini^{73a}, A.S. Chisholm¹⁸, R.T. Chislett⁷⁸, A. Chitan^{26b},
 M.V. Chizhov⁶⁵, K. Choi⁶¹, S. Chouridou⁹, B.K.B. Chow¹⁰⁰, V. Christodoulou⁷⁸, D. Chromek-Burckhart³⁰,
 J. Chudoba¹²⁷, A.J. Chuinard⁸⁷, J.J. Chwastowski³⁹, L. Chytka¹¹⁵, G. Ciapetti^{132a,132b}, A.K. Ciftci^{4a},
 D. Cinca⁵³, V. Cindro⁷⁵, I.A. Cioara²¹, A. Ciochio¹⁵, F. Ciroto^{104a,104b}, Z.H. Citron¹⁷², M. Ciubancan^{26b},
 A. Clark⁴⁹, B.L. Clark⁵⁷, P.J. Clark⁴⁶, R.N. Clarke¹⁵, C. Clement^{146a,146b}, Y. Coadou⁸⁵, M. Cokal^{164a,164c},
 A. Coccaro⁴⁹, J. Cochran⁶⁴, L. Coffey²³, J.G. Cogan¹⁴³, L. Colasurdo¹⁰⁶, B. Cole³⁵, S. Cole¹⁰⁸,
 A.P. Colijn¹⁰⁷, J. Collot⁵⁵, T. Colombo^{58c}, G. Compostella¹⁰¹, P. Conde Muiño^{126a,126b}, E. Coniavitis⁴⁸,
 S.H. Connell^{145b}, I.A. Connelly⁷⁷, V. Consorti⁴⁸, S. Constantinescu^{26b}, C. Conta^{121a,121b}, G. Conti³⁰,
 F. Conventi^{104a,j}, M. Cooke¹⁵, B.D. Cooper⁷⁸, A.M. Cooper-Sarkar¹²⁰, T. Cornelissen¹⁷⁵, M. Corradi^{20a},
 F. Corriveau^{87,k}, A. Corso-Radu¹⁶³, A. Cortes-Gonzalez¹², G. Cortiana¹⁰¹, G. Costa^{91a}, M.J. Costa¹⁶⁷,
 D. Costanzo¹³⁹, D. Côté⁸, G. Cottin²⁸, G. Cowan⁷⁷, B.E. Cox⁸⁴, K. Cranmer¹¹⁰, G. Cree²⁹,
 S. Crépe-Renaudin⁵⁵, F. Crescioli⁸⁰, W.A. Cribbs^{146a,146b}, M. Crispin Ortuzar¹²⁰, M. Cristinziani²¹,
 V. Croft¹⁰⁶, G. Crosetti^{37a,37b}, T. Cuhadar Donszelmann¹³⁹, J. Cummings¹⁷⁶, M. Curatolo⁴⁷, J. Cúth⁸³,
 C. Cuthbert¹⁵⁰, H. Czirr¹⁴¹, P. Czodrowski³, S. D'Auria⁵³, M. D'Onofrio⁷⁴,
 M.J. Da Cunha Sargedas De Sousa^{126a,126b}, C. Da Via⁸⁴, W. Dabrowski^{38a}, A. Dainca¹²⁰, T. Dai⁸⁹,
 O. Dale¹⁴, F. Dallaire⁹⁵, C. Dallapiccola⁸⁶, M. Dam³⁶, J.R. Dandoy³¹, N.P. Dang⁴⁸, A.C. Daniells¹⁸,
 M. Danninger¹⁶⁸, M. Dano Hoffmann¹³⁶, V. Dao⁴⁸, G. Darbo^{50a}, S. Darmora⁸, J. Dassoulas³,
 A. Dattagupta⁶¹, W. Davey²¹, C. David¹⁶⁹, T. Davidek¹²⁹, E. Davies^{120,l}, M. Davies¹⁵³, P. Davison⁷⁸,
 Y. Davygora^{58a}, E. Dawe⁸⁸, I. Dawson¹³⁹, R.K. Daya-Ishmukhametova⁸⁶, K. De⁸, R. de Asmundis^{104a},
 A. De Benedetti¹¹³, S. De Castro^{20a,20b}, S. De Cecco⁸⁰, N. De Groot¹⁰⁶, P. de Jong¹⁰⁷, H. De la Torre⁸²,
 F. De Lorenzi⁶⁴, D. De Pedis^{132a}, A. De Salvo^{132a}, U. De Sanctis¹⁴⁹, A. De Santo¹⁴⁹,
 J.B. De Vivie De Regie¹¹⁷, W.J. Dearnaley⁷², R. Debe²⁵, C. Debenedetti¹³⁷, D.V. Dedovich⁶⁵,
 I. Deigaard¹⁰⁷, J. Del Peso⁸², T. Del Prete^{124a,124b}, D. Delgove¹¹⁷, F. Deliot¹³⁶, C.M. Delitzsch⁴⁹,
 M. Deliyergiyev⁷⁵, A. Dell'Acqua³⁰, L. Dell'Asta²², M. Dell'Orso^{124a,124b}, M. Della Pietra^{104a,j},
 D. della Volpe⁴⁹, M. Delmastro⁵, P.A. Delsart⁵⁵, C. Deluca¹⁰⁷, D.A. DeMarco¹⁵⁸, S. Demers¹⁷⁶,
 M. Demichev⁶⁵, A. Demilly⁸⁰, S.P. Denisov¹³⁰, D. Derendarz³⁹, J.E. Derkaoui^{135d}, F. Derue⁸⁰,
 P. Dervan⁷⁴, K. Desch²¹, C. Deterre⁴², K. Dette⁴³, P.O. Deviveiros³⁰, A. Dewhurst¹³¹, S. Dhaliwal²³,
 A. Di Ciaccio^{133a,133b}, L. Di Ciaccio⁵, A. Di Domenico^{132a,132b}, C. Di Donato^{104a,104b}, A. Di Girolamo³⁰,
 B. Di Girolamo³⁰, A. Di Mattia¹⁵², B. Di Micco^{134a,134b}, R. Di Nardo⁴⁷, A. Di Simone⁴⁸, R. Di Sipio¹⁵⁸,
 D. Di Valentino²⁹, C. Diaconu⁸⁵, M. Diamond¹⁵⁸, F.A. Dias⁴⁶, M.A. Diaz^{32a}, E.B. Diehl⁸⁹, J. Dietrich¹⁶,
 S. Diglio⁸⁵, A. Dimitrievska¹³, J. Dingfelder²¹, P. Dita^{26b}, S. Dita^{26b}, F. Dittus³⁰, F. Djama⁸⁵,
 T. Djobava^{51b}, J.I. Djuvsland^{58a}, M.A.B. do Vale^{24c}, D. Dobos³⁰, M. Dobre^{26b}, C. Doglioni⁸¹,
 T. Dohmae¹⁵⁵, J. Dolejsi¹²⁹, Z. Dolezal¹²⁹, B.A. Dolgoshein^{98,*}, M. Donadelli^{24d}, S. Donati^{124a,124b},
 P. Dondero^{121a,121b}, J. Donini³⁴, J. Dopke¹³¹, A. Doria^{104a}, M.T. Dova⁷¹, A.T. Doyle⁵³, E. Drechsler⁵⁴,
 M. Dris¹⁰, E. Dubreuil³⁴, E. Duchovni¹⁷², G. Duckeck¹⁰⁰, O.A. Ducu^{26b,85}, D. Duda¹⁰⁷, A. Dudarev³⁰,
 L. Duflot¹¹⁷, L. Duguid⁷⁷, M. Dührssen³⁰, M. Dunford^{58a}, H. Duran Yildiz^{4a}, M. Düren⁵²,
 A. Durglishvili^{51b}, D. Duschinger⁴⁴, B. Dutta⁴², M. Dyndal^{38a}, C. Eckardt⁴², K.M. Ecker¹⁰¹, R.C. Edgar⁸⁹,
 W. Edson², N.C. Edwards⁴⁶, W. Ehrenfeld²¹, T. Eifert³⁰, G. Eigen¹⁴, K. Einsweiler¹⁵, T. Ekelof¹⁶⁶,
 M. El Kacimi^{135c}, M. Ellert¹⁶⁶, S. Elles⁵, F. Ellinghaus¹⁷⁵, A.A. Elliot¹⁶⁹, N. Ellis³⁰, J. Elmsheuser¹⁰⁰,
 M. Elsing³⁰, D. Emelianov¹³¹, Y. Enari¹⁵⁵, O.C. Endner⁸³, M. Endo¹¹⁸, J. Erdmann⁴³, A. Ereditato¹⁷,
 G. Ernis¹⁷⁵, J. Ernst², M. Ernst²⁵, S. Errede¹⁶⁵, E. Ertel⁸³, M. Escalier¹¹⁷, H. Esch⁴³, C. Escobar¹²⁵,
 B. Esposito⁴⁷, A.I. Etiennevre¹³⁶, E. Etzion¹⁵³, H. Evans⁶¹, A. Ezhilov¹²³, L. Fabbri^{20a,20b}, G. Facini³¹,
 R.M. Fakhruddinov¹³⁰, S. Falciano^{132a}, R.J. Falla⁷⁸, J. Faltova¹²⁹, Y. Fang^{33a}, M. Fanti^{91a,91b}, A. Farbin⁸,
 A. Farilla^{134a}, T. Farooque¹², S. Farrell¹⁵, S.M. Farrington¹⁷⁰, P. Farthouat³⁰, F. Fassi^{135e}, P. Fassnacht³⁰,
 D. Fassouliotis⁹, M. Faucci Giannelli⁷⁷, A. Favareto^{50a,50b}, L. Fayard¹¹⁷, O.L. Fedin^{123,m}, W. Fedorko¹⁶⁸,
 S. Feigl³⁰, L. Felgioni⁸⁵, C. Feng^{33d}, E.J. Feng³⁰, H. Feng⁸⁹, A.B. Fenyuk¹³⁰, L. Feremenga⁸,
 P. Fernandez Martinez¹⁶⁷, S. Fernandez Perez³⁰, J. Ferrando⁵³, A. Ferrari¹⁶⁶, P. Ferrari¹⁰⁷, R. Ferrari^{121a},
 D.E. Ferreira de Lima⁵³, A. Ferrer¹⁶⁷, D. Ferrere⁴⁹, C. Ferretti⁸⁹, A. Ferretto Parodi^{50a,50b}, M. Fiascaris³¹,

F. Fiedler⁸³, A. Filipčič⁷⁵, M. Filipuzzi⁴², F. Filthaut¹⁰⁶, M. Fincke-Keeler¹⁶⁹, K.D. Finelli¹⁵⁰, M.C.N. Fiolhais^{126a,126c}, L. Fiorini¹⁶⁷, A. Firan⁴⁰, A. Fischer², C. Fischer¹², J. Fischer¹⁷⁵, W.C. Fisher⁹⁰, N. Flaschel⁴², I. Fleck¹⁴¹, P. Fleischmann⁸⁹, G.T. Fletcher¹³⁹, G. Fletcher⁷⁶, R.R.M. Fletcher¹²², T. Flick¹⁷⁵, A. Floderus⁸¹, L.R. Flores Castillo^{60a}, M.J. Flowerdew¹⁰¹, A. Formica¹³⁶, A. Forti⁸⁴, D. Fournier¹¹⁷, H. Fox⁷², S. Fracchia¹², P. Francavilla⁸⁰, M. Franchini^{20a,20b}, D. Francis³⁰, L. Franconi¹¹⁹, M. Franklin⁵⁷, M. Frate¹⁶³, M. Fraternali^{121a,121b}, D. Freeborn⁷⁸, S.T. French²⁸, F. Friedrich⁴⁴, D. Froidevaux³⁰, J.A. Frost¹²⁰, C. Fukunaga¹⁵⁶, E. Fullana Torregrosa⁸³, B.G. Fulson¹⁴³, T. Fusayasu¹⁰², J. Fuster¹⁶⁷, C. Gabaldon⁵⁵, O. Gabizon¹⁷⁵, A. Gabrielli^{20a,20b}, A. Gabrielli¹⁵, G.P. Gach¹⁸, S. Gadatsch³⁰, S. Gadomski⁴⁹, G. Gagliardi^{50a,50b}, P. Gagnon⁶¹, C. Galea¹⁰⁶, B. Galhardo^{126a,126c}, E.J. Gallas¹²⁰, B.J. Gallop¹³¹, P. Gallus¹²⁸, G. Galster³⁶, K.K. Gan¹¹¹, J. Gao^{33b,85}, Y. Gao⁴⁶, Y.S. Gao^{143,e}, F.M. Garay Walls⁴⁶, F. Garberon¹⁷⁶, C. García¹⁶⁷, J.E. García Navarro¹⁶⁷, M. Garcia-Sciveres¹⁵, R.W. Gardner³¹, N. Garelli¹⁴³, V. Garonne¹¹⁹, C. Gatti⁴⁷, A. Gaudiello^{50a,50b}, G. Gaudio^{121a}, B. Gaur¹⁴¹, L. Gauthier⁹⁵, P. Gauzzi^{132a,132b}, I.L. Gavrilenko⁹⁶, C. Gay¹⁶⁸, G. Gaycken²¹, E.N. Gazis¹⁰, P. Ge^{33d}, Z. Gece¹⁶⁸, C.N.P. Gee¹³¹, Ch. Geich-Gimbel²¹, M.P. Geisler^{58a}, C. Gemme^{50a}, M.H. Genest⁵⁵, S. Gentile^{132a,132b}, M. George⁵⁴, S. George⁷⁷, D. Gerbaudo¹⁶³, A. Gershon¹⁵³, S. Ghasemi¹⁴¹, H. Ghazlane^{135b}, B. Giacobbe^{20a}, S. Giagu^{132a,132b}, V. Giangiobbe¹², P. Giannetti^{124a,124b}, B. Gibbard²⁵, S.M. Gibson⁷⁷, M. Gignac¹⁶⁸, M. Gilchriese¹⁵, T.P.S. Gillam²⁸, D. Gillberg³⁰, G. Gilles³⁴, D.M. Gingrich^{3,d}, N. Giokaris⁹, M.P. Giordani^{164a,164c}, F.M. Giorgi^{20a}, F.M. Giorgi¹⁶, P.F. Giraud¹³⁶, P. Giromini⁴⁷, D. Giugni^{91a}, C. Giuliani¹⁰¹, M. Giulini^{58b}, B.K. Gjelsten¹¹⁹, S. Gkaitatzis¹⁵⁴, I. Gkialas¹⁵⁴, E.L. Gkoukousis¹¹⁷, L.K. Gladilin⁹⁹, C. Glasman⁸², J. Glatzer³⁰, P.C.F. Glaysher⁴⁶, A. Glazov⁴², M. Goblirsch-Kolb¹⁰¹, J.R. Goddard⁷⁶, J. Godlewski³⁹, S. Goldfarb⁸⁹, T. Golling⁴⁹, D. Golubkov¹³⁰, A. Gomes^{126a,126b,126d}, R. Gonçalves^{126a}, J. Goncalves Pinto Firmino Da Costa¹³⁶, L. Gonella²¹, S. González de la Hoz¹⁶⁷, G. Gonzalez Parra¹², S. Gonzalez-Sevilla⁴⁹, L. Goossens³⁰, P.A. Gorbounov⁹⁷, H.A. Gordon²⁵, I. Gorelov¹⁰⁵, B. Gorini³⁰, E. Gorini^{73a,73b}, A. Gorišek⁷⁵, E. Gornicki³⁹, A.T. Goshaw⁴⁵, C. Gössling⁴³, M.I. Gostkin⁶⁵, D. Goujdami^{135c}, A.G. Goussiou¹³⁸, N. Govender^{145b}, E. Gozani¹⁵², H.M.X. Grabas¹³⁷, L. Graber⁵⁴, I. Grabowska-Bold^{38a}, P.O.J. Gradin¹⁶⁶, P. Grafström^{20a,20b}, K.-J. Grahn⁴², J. Gramling⁴⁹, E. Gramstad¹¹⁹, S. Grancagnolo¹⁶, V. Gratchev¹²³, H.M. Gray³⁰, E. Graziani^{134a}, Z.D. Greenwood^{79,n}, C. Grefe²¹, K. Gregersen⁷⁸, I.M. Gregor⁴², P. Grenier¹⁴³, J. Griffiths⁸, A.A. Grillo¹³⁷, K. Grimm⁷², S. Grinstein^{12,o}, Ph. Gris³⁴, J.-F. Grivaz¹¹⁷, J.P. Grohs⁴⁴, A. Grohsjean⁴², E. Gross¹⁷², J. Grosse-Knetter⁵⁴, G.C. Grossi⁷⁹, Z.J. Grout¹⁴⁹, L. Guan⁸⁹, J. Guenther¹²⁸, F. Guescini⁴⁹, D. Guest¹⁶³, O. Gueta¹⁵³, E. Guido^{50a,50b}, T. Guillemin¹¹⁷, S. Guindon², U. Gul⁵³, C. Gumpert⁴⁴, J. Guo^{33e}, Y. Guo^{33b,p}, S. Gupta¹²⁰, G. Gustavino^{132a,132b}, P. Gutierrez¹¹³, N.G. Gutierrez Ortiz⁷⁸, C. Gutschow⁴⁴, C. Guyot¹³⁶, C. Gwenlan¹²⁰, C.B. Gwilliam⁷⁴, A. Haas¹¹⁰, C. Haber¹⁵, H.K. Hadavand⁸, N. Haddad^{135e}, P. Haefner²¹, S. Hageböck²¹, Z. Hajduk³⁹, H. Hakobyan¹⁷⁷, M. Haleem⁴², J. Haley¹¹⁴, D. Hall¹²⁰, G. Halladjian⁹⁰, G.D. Hallowell⁸⁵, K. Hamacher¹⁷⁵, P. Hamal¹¹⁵, K. Hamano¹⁶⁹, A. Hamilton^{145a}, G.N. Hamity¹³⁹, P.G. Hamnett⁴², L. Han^{33b}, K. Hanagaki^{66,q}, K. Hanawa¹⁵⁵, M. Hance¹³⁷, B. Haney¹²², P. Hanke^{58a}, R. Hanna¹³⁶, J.B. Hansen³⁶, J.D. Hansen³⁶, M.C. Hansen²¹, P.H. Hansen³⁶, K. Hara¹⁶⁰, A.S. Hard¹⁷³, T. Harenberg¹⁷⁵, F. Hariri¹¹⁷, S. Harkusha⁹², R.D. Harrington⁴⁶, P.F. Harrison¹⁷⁰, F. Hartjes¹⁰⁷, M. Hasegawa⁶⁷, Y. Hasegawa¹⁴⁰, A. Hasib¹¹³, S. Hassani¹³⁶, S. Haug¹⁷, R. Hauser⁹⁰, L. Hauswald⁴⁴, M. Havranek¹²⁷, C.M. Hawkes¹⁸, R.J. Hawkings³⁰, A.D. Hawkins⁸¹, T. Hayashi¹⁶⁰, D. Hayden⁹⁰, C.P. Hays¹²⁰, J.M. Hays⁷⁶, H.S. Hayward⁷⁴, S.J. Haywood¹³¹, S.J. Head¹⁸, T. Heck⁸³, V. Hedberg⁸¹, L. Heelan⁸, S. Heim¹²², T. Heim¹⁷⁵, B. Heinemann¹⁵, L. Heinrich¹¹⁰, J. Hejbal¹²⁷, L. Helary²², S. Hellman^{146a,146b}, D. Hellmich²¹, C. Helsens¹², J. Henderson¹²⁰, R.C.W. Henderson⁷², Y. Heng¹⁷³, C. Hengler⁴², S. Henkelmann¹⁶⁸, A. Henrichs¹⁷⁶, A.M. Henriques Correia³⁰, S. Henrot-Versille¹¹⁷, G.H. Herbert¹⁶, Y. Hernández Jiménez¹⁶⁷, G. Herten⁴⁸, R. Hertenberger¹⁰⁰, L. Hervas³⁰, G.G. Hesketh⁷⁸, N.P. Hessey¹⁰⁷, J.W. Hetherly⁴⁰, R. Hickling⁷⁶, E. Higón-Rodríguez¹⁶⁷, E. Hill¹⁶⁹, J.C. Hill²⁸, K.H. Hiller⁴², S.J. Hillier¹⁸, I. Hinchliffe¹⁵, E. Hines¹²², R.R. Hinman¹⁵, M. Hirose¹⁵⁷, D. Hirschbuehl¹⁷⁵, J. Hobbs¹⁴⁸, N. Hod¹⁰⁷, M.C. Hodgkinson¹³⁹, P. Hodgson¹³⁹, A. Hoecker³⁰, M.R. Hoferkamp¹⁰⁵, F. Hoenic¹⁰⁰, M. Hohlfield⁸³, D. Hohn²¹, T.R. Holmes¹⁵, M. Homann⁴³, T.M. Hong¹²⁵, W.H. Hopkins¹¹⁶, Y. Horii¹⁰³, A.J. Horton¹⁴², J.-Y. Hostachy⁵⁵, S. Hou¹⁵¹, A. Hoummada^{135a}, J. Howard¹²⁰, J. Howarth⁴², M. Hrabovsky¹¹⁵, I. Hristova¹⁶, J. Hrivnac¹¹⁷, T. Hryn'ova⁵, A. Hrynevich⁹³, C. Hsu^{145c}, P.J. Hsu^{151,r}, S.-C. Hsu¹³⁸, D. Hu³⁵, Q. Hu^{33b}, X. Hu⁸⁹,

Y. Huang⁴², Z. Hubacek¹²⁸, F. Hubaut⁸⁵, F. Huegging²¹, T.B. Huffman¹²⁰, E.W. Hughes³⁵, G. Hughes⁷²,
 M. Huhtinen³⁰, T.A. Hülsing⁸³, N. Huseynov^{65,b}, J. Huston⁹⁰, J. Huth⁵⁷, G. Iacobucci⁴⁹, G. Iakovidis²⁵,
 I. Ibragimov¹⁴¹, L. Iconomidou-Fayard¹¹⁷, E. Ideal¹⁷⁶, Z. Idrissi^{135e}, P. Iengo³⁰, O. Igonkina¹⁰⁷,
 T. Iizawa¹⁷¹, Y. Ikegami⁶⁶, K. Ikematsu¹⁴¹, M. Ikeno⁶⁶, Y. Ilchenko^{31,s}, D. Iliadis¹⁵⁴, N. Ilic¹⁴³,
 T. Ince¹⁰¹, G. Introzzi^{121a,121b}, P. Ioannou⁹, M. Iodice^{134a}, K. Iordanidou³⁵, V. Ippolito⁵⁷,
 A. Irlles Quiles¹⁶⁷, C. Isaksson¹⁶⁶, M. Ishino⁶⁸, M. Ishitsuka¹⁵⁷, R. Ishmukhametov¹¹¹, C. Issever¹²⁰,
 S. Istin^{19a}, J.M. Iturbe Ponce⁸⁴, R. Iuppa^{133a,133b}, J. Ivarsson⁸¹, W. Iwanski³⁹, H. Iwasaki⁶⁶, J.M. Izen⁴¹,
 V. Izzo^{104a}, S. Jabbar³, B. Jackson¹²², M. Jackson⁷⁴, P. Jackson¹, M.R. Jaekel³⁰, V. Jain², K. Jakobs⁴⁸,
 S. Jakobsen³⁰, T. Jakoubek¹²⁷, J. Jakubek¹²⁸, D.O. Jamin¹¹⁴, D.K. Jana⁷⁹, E. Jansen⁷⁸, R. Jansky⁶²,
 J. Janssen²¹, M. Janus⁵⁴, G. Jarlskog⁸¹, N. Javadov^{65,b}, T. Javůrek⁴⁸, L. Jeanty¹⁵, J. Jejelava^{51a,t},
 G.-Y. Jeng¹⁵⁰, D. Jennens⁸⁸, P. Jenni^{48,u}, J. Jentsch⁴³, C. Jeske¹⁷⁰, S. Jézéquel⁵, H. Ji¹⁷³, J. Jia¹⁴⁸,
 Y. Jiang^{33b}, S. Jiggins⁷⁸, J. Jimenez Pena¹⁶⁷, S. Jin^{33a}, A. Jinaru^{26b}, O. Jinnouchi¹⁵⁷, M.D. Joergensen³⁶,
 P. Johansson¹³⁹, K.A. Johns⁷, W.J. Johnson¹³⁸, K. Jon-And^{146a,146b}, G. Jones¹⁷⁰, R.W.L. Jones⁷²,
 T.J. Jones⁷⁴, J. Jongmanns^{58a}, P.M. Jorge^{126a,126b}, K.D. Joshi⁸⁴, J. Jovicevic^{159a}, X. Ju¹⁷³, P. Jussel⁶²,
 A. Juste Rozas^{12,o}, M. Kaci¹⁶⁷, A. Kaczmarska³⁹, M. Kado¹¹⁷, H. Kagan¹¹¹, M. Kagan¹⁴³, S.J. Kahn⁸⁵,
 E. Kajomovitz⁴⁵, C.W. Kalderon¹²⁰, S. Kama⁴⁰, A. Kamenshchikov¹³⁰, N. Kanaya¹⁵⁵, S. Kaneti²⁸,
 V.A. Kantserov⁹⁸, J. Kanzaki⁶⁶, B. Kaplan¹¹⁰, L.S. Kaplan¹⁷³, A. Kapliy³¹, D. Kar^{145c}, K. Karakostas¹⁰,
 A. Karamaoun³, N. Karastathis^{10,107}, M.J. Kareem⁵⁴, E. Karentzos¹⁰, M. Karnevskiy⁸³, S.N. Karpov⁶⁵,
 Z.M. Karpova⁶⁵, K. Karthik¹¹⁰, V. Kartvelishvili⁷², A.N. Karyukhin¹³⁰, K. Kasahara¹⁶⁰, L. Kashif¹⁷³,
 R.D. Kass¹¹¹, A. Kastanas¹⁴, Y. Kataoka¹⁵⁵, C. Kato¹⁵⁵, A. Katre⁴⁹, J. Katzy⁴², K. Kawade¹⁰³,
 K. Kawagoe⁷⁰, T. Kawamoto¹⁵⁵, G. Kawamura⁵⁴, S. Kazama¹⁵⁵, V.F. Kazanin^{109,c}, R. Keeler¹⁶⁹,
 R. Kehoe⁴⁰, J.S. Keller⁴², J.J. Kempster⁷⁷, H. Keoshkerian⁸⁴, O. Kepka¹²⁷, B.P. Kerševan⁷⁵, S. Kersten¹⁷⁵,
 R.A. Keyes⁸⁷, F. Khalil-zada¹¹, H. Khandanyan^{146a,146b}, A. Khanov¹¹⁴, A.G. Kharlamov^{109,c}, T.J. Khoo²⁸,
 V. Khovanskiy⁹⁷, E. Khramov⁶⁵, J. Khubua^{51b,v}, S. Kido⁶⁷, H.Y. Kim⁸, S.H. Kim¹⁶⁰, Y.K. Kim³¹,
 N. Kimura¹⁵⁴, O.M. Kind¹⁶, B.T. King⁷⁴, M. King¹⁶⁷, S.B. King¹⁶⁸, J. Kirk¹³¹, A.E. Kiryunin¹⁰¹,
 T. Kishimoto⁶⁷, D. Kisielewska^{38a}, F. Kiss⁴⁸, K. Kiuchi¹⁶⁰, O. Kivernyk¹³⁶, E. Kladiva^{144b}, M.H. Klein³⁵,
 M. Klein⁷⁴, U. Klein⁷⁴, K. Kleinknecht⁸³, P. Klimek^{146a,146b}, A. Klimentov²⁵, R. Klingenberg⁴³,
 J.A. Klinger¹³⁹, T. Klioutchnikova³⁰, E.-E. Kluge^{58a}, P. Kluit¹⁰⁷, S. Kluth¹⁰¹, J. Knapik³⁹, E. Kneringer⁶²,
 E.B.F.G. Knoop⁸⁵, A. Knue⁵³, A. Kobayashi¹⁵⁵, D. Kobayashi¹⁵⁷, T. Kobayashi¹⁵⁵, M. Kobel⁴⁴,
 M. Kocian¹⁴³, P. Kodys¹²⁹, T. Koffas²⁹, E. Koffeman¹⁰⁷, L.A. Kogan¹²⁰, S. Kohlmann¹⁷⁵, Z. Kohout¹²⁸,
 T. Kohriki⁶⁶, T. Koi¹⁴³, H. Kolanoski¹⁶, M. Kolb^{58b}, I. Koletsou⁵, A.A. Komar^{96,*}, Y. Komori¹⁵⁵,
 T. Kondo⁶⁶, N. Kondrashova⁴², K. Köneke⁴⁸, A.C. König¹⁰⁶, T. Kono⁶⁶, R. Konoplich^{110,w},
 N. Konstantinidis⁷⁸, R. Kopeliansky¹⁵², S. Koperny^{38a}, L. Köpke⁸³, A.K. Kopp⁴⁸, K. Korcyl³⁹,
 K. Kordas¹⁵⁴, A. Korn⁷⁸, A.A. Korol^{109,c}, I. Korolkov¹², E.V. Korolkova¹³⁹, O. Kortner¹⁰¹, S. Kortner¹⁰¹,
 T. Kosek¹²⁹, V.V. Kostyukhin²¹, V.M. Kotov⁶⁵, A. Kotwal⁴⁵, A. Kourkoumeli-Charalampidi¹⁵⁴,
 C. Kourkoumelis⁹, V. Kouskoura²⁵, A. Koutsman^{159a}, R. Kowalewski¹⁶⁹, T.Z. Kowalski^{38a},
 W. Kozanecki¹³⁶, A.S. Kozhin¹³⁰, V.A. Kramarenko⁹⁹, G. Kramberger⁷⁵, D. Krasnopevtsev⁹⁸,
 M.W. Krasny⁸⁰, A. Krasznahorkay³⁰, J.K. Kraus²¹, A. Kravchenko²⁵, S. Kreiss¹¹⁰, M. Kretz^{58c},
 J. Kretzschmar⁷⁴, K. Kreutzfeldt⁵², P. Krieger¹⁵⁸, K. Krizka³¹, K. Kroeninger⁴³, H. Kroha¹⁰¹, J. Kroll¹²²,
 J. Kröseberg²¹, J. Krstic¹³, U. Kruchonak⁶⁵, H. Krüger²¹, N. Krumnack⁶⁴, A. Kruse¹⁷³, M.C. Kruse⁴⁵,
 M. Kruskal²², T. Kubota⁸⁸, H. Kucuk⁷⁸, S. Kuday^{4b}, S. Kuehn⁴⁸, A. Kugel^{58c}, F. Kuger¹⁷⁴, A. Kuhl¹³⁷,
 T. Kuhl⁴², V. Kukhtin⁶⁵, R. Kukla¹³⁶, Y. Kulchitsky⁹², S. Kuleshov^{32b}, M. Kuna^{132a,132b}, T. Kunigo⁶⁸,
 A. Kupco¹²⁷, H. Kurashige⁶⁷, Y.A. Kurochkin⁹², V. Kus¹²⁷, E.S. Kuwertz¹⁶⁹, M. Kuze¹⁵⁷, J. Kvita¹¹⁵,
 T. Kwan¹⁶⁹, D. Kyriazopoulos¹³⁹, A. La Rosa¹³⁷, J.L. La Rosa Navarro^{24d}, L. La Rotonda^{37a,37b},
 C. Lacasta¹⁶⁷, F. Lacava^{132a,132b}, J. Lacey²⁹, H. Lacker¹⁶, D. Lacour⁸⁰, V.R. Lacuesta¹⁶⁷, E. Ladygin⁶⁵,
 R. Lafaye⁵, B. Laforge⁸⁰, T. Lagouri¹⁷⁶, S. Lai⁵⁴, L. Lambourne⁷⁸, S. Lammers⁶¹, C.L. Lampen⁷,
 W. Lampl⁷, E. Lançon¹³⁶, U. Landgraf⁴⁸, M.P.J. Landon⁷⁶, V.S. Lang^{58a}, J.C. Lange¹², A.J. Lankford¹⁶³,
 F. Lanni²⁵, K. Lantzsch²¹, A. Lanza^{121a}, S. Laplace⁸⁰, C. Lapoire³⁰, J.F. Laporte¹³⁶, T. Lari^{91a},
 F. Lasagni Manghi^{20a,20b}, M. Lassnig³⁰, P. Laurelli⁴⁷, W. Lavrijsen¹⁵, A.T. Law¹³⁷, P. Laycock⁷⁴,
 T. Lazovich⁵⁷, O. Le Dortz⁸⁰, E. Le Guirriec⁸⁵, E. Le Menedeu¹², M. LeBlanc¹⁶⁹, T. LeCompte⁶,
 F. Ledroit-Guillon⁵⁵, C.A. Lee^{145a}, S.C. Lee¹⁵¹, L. Lee¹, G. Lefebvre⁸⁰, M. Lefebvre¹⁶⁹, F. Legger¹⁰⁰,
 C. Leggett¹⁵, A. Lehan⁷⁴, G. Lehmann Miotto³⁰, X. Lei⁷, W.A. Leight²⁹, A. Leisos^{154,x}, A.G. Leister¹⁷⁶,

M.A.L. Leite^{24d}, R. Leitner¹²⁹, D. Lellouch¹⁷², B. Lemmer⁵⁴, K.J.C. Leney⁷⁸, T. Lenz²¹, B. Lenzi³⁰,
 R. Leone⁷, S. Leone^{124a,124b}, C. Leonidopoulos⁴⁶, S. Leontsinis¹⁰, C. Leroy⁹⁵, C.G. Lester²⁸,
 M. Levchenko¹²³, J. Levêque⁵, D. Levin⁸⁹, L.J. Levinson¹⁷², M. Levy¹⁸, A. Lewis¹²⁰, A.M. Leyko²¹,
 M. Leyton⁴¹, B. Li^{33b,y}, H. Li¹⁴⁸, H.L. Li³¹, L. Li⁴⁵, L. Li^{33e}, S. Li⁴⁵, X. Li⁸⁴, Y. Li^{33c,z}, Z. Liang¹³⁷,
 H. Liao³⁴, B. Liberti^{133a}, A. Liblong¹⁵⁸, P. Lichard³⁰, K. Lie¹⁶⁵, J. Liebal²¹, W. Liebig¹⁴, C. Limbach²¹,
 A. Limosani¹⁵⁰, S.C. Lin^{151,aa}, T.H. Lin⁸³, F. Linde¹⁰⁷, B.E. Lindquist¹⁴⁸, J.T. Linnemann⁹⁰, E. Lipeles¹²²,
 A. Lipniacka¹⁴, M. Lisovsky^{58b}, T.M. Liss¹⁶⁵, D. Lissauer²⁵, A. Lister¹⁶⁸, A.M. Litke¹³⁷, B. Liu^{151,ab},
 D. Liu¹⁵¹, H. Liu⁸⁹, J. Liu⁸⁵, J.B. Liu^{33b}, K. Liu⁸⁵, L. Liu¹⁶⁵, M. Liu⁴⁵, M. Liu^{33b}, Y. Liu^{33b},
 M. Livan^{121a,121b}, A. Lleres⁵⁵, J. Llorente Merino⁸², S.L. Lloyd⁷⁶, F. Lo Sterzo¹⁵¹, E. Lobodzinska⁴²,
 P. Loch⁷, W.S. Lockman¹³⁷, F.K. Loebinger⁸⁴, A.E. Loevschall-Jensen³⁶, K.M. Loew²³, A. Loginov¹⁷⁶,
 T. Lohse¹⁶, K. Lohwasser⁴², M. Lokajicek¹²⁷, B.A. Long²², J.D. Long¹⁶⁵, R.E. Long⁷², K.A. Looper¹¹¹,
 L. Lopes^{126a}, D. Lopez Mateos⁵⁷, B. Lopez Paredes¹³⁹, I. Lopez Paz¹², J. Lorenz¹⁰⁰,
 N. Lorenzo Martinez⁶¹, M. Losada¹⁶², P.J. Lösel¹⁰⁰, X. Lou^{33a}, A. Lounis¹¹⁷, J. Love⁶, P.A. Love⁷²,
 H. Lu^{60a}, N. Lu⁸⁹, H.J. Lubatti¹³⁸, C. Luci^{132a,132b}, A. Lucotte⁵⁵, C. Luedtke⁴⁸, F. Luehring⁶¹, W. Lukas⁶²,
 L. Luminari^{132a}, O. Lundberg^{146a,146b}, B. Lund-Jensen¹⁴⁷, D. Lynn²⁵, R. Lysak¹²⁷, E. Lytken⁸¹, H. Ma²⁵,
 L.L. Ma^{33d}, G. Maccarrone⁴⁷, A. Macchiolo¹⁰¹, C.M. Macdonald¹³⁹, B. Maček⁷⁵,
 J. Machado Miguens^{122,126b}, D. Macina³⁰, D. Madaffari⁸⁵, R. Madar³⁴, H.J. Maddocks⁷², W.F. Mader⁴⁴,
 A. Madsen¹⁶⁶, J. Maeda⁶⁷, S. Maeland¹⁴, T. Maeno²⁵, A. Maevskiy⁹⁹, E. Magradze⁵⁴, K. Mahboubi⁴⁸,
 J. Mahlstedt¹⁰⁷, C. Maiani¹³⁶, C. Maidantchik^{24a}, A.A. Maier¹⁰¹, T. Maier¹⁰⁰, A. Maio^{126a,126b,126d},
 S. Majewski¹¹⁶, Y. Makida⁶⁶, N. Makovec¹¹⁷, B. Malaescu⁸⁰, Pa. Malecki³⁹, V.P. Maleev¹²³, F. Malek⁵⁵,
 U. Mallik⁶³, D. Malon⁶, C. Malone¹⁴³, S. Maltezos¹⁰, V.M. Malyshev¹⁰⁹, S. Malyukov³⁰, J. Mamuzic⁴²,
 G. Mancini⁴⁷, B. Mandelli³⁰, L. Mandelli^{91a}, I. Mandić⁷⁵, R. Mandrysch⁶³, J. Maneira^{126a,126b},
 A. Manfredini¹⁰¹, L. Manhaes de Andrade Filho^{24b}, J. Manjarres Ramos^{159b}, A. Mann¹⁰⁰,
 A. Manousakis-Katsikakis⁹, B. Mansoulie¹³⁶, R. Mantifel⁸⁷, M. Mantoani⁵⁴, L. Mapelli³⁰, L. March^{145c},
 G. Marchiori⁸⁰, M. Marcisovsky¹²⁷, C.P. Marino¹⁶⁹, M. Marjanovic¹³, D.E. Marley⁸⁹, F. Marroquim^{24a},
 S.P. Marsden⁸⁴, Z. Marshall¹⁵, L.F. Marti¹⁷, S. Marti-Garcia¹⁶⁷, B. Martin⁹⁰, T.A. Martin¹⁷⁰, V.J. Martin⁴⁶,
 B. Martin dit Latour¹⁴, M. Martinez^{12,o}, S. Martin-Haugh¹³¹, V.S. Martoiu^{26b}, A.C. Martyniuk⁷⁸,
 M. Marx¹³⁸, F. Marzano^{132a}, A. Marzin³⁰, L. Masetti⁸³, T. Mashimo¹⁵⁵, R. Mashinistov⁹⁶, J. Masik⁸⁴,
 A.L. Maslennikov^{109,c}, I. Massa^{20a,20b}, L. Massa^{20a,20b}, P. Mastrandrea⁵, A. Mastroberardino^{37a,37b},
 T. Masubuchi¹⁵⁵, P. Mättig¹⁷⁵, J. Mattmann⁸³, J. Maurer^{26b}, S.J. Maxfield⁷⁴, D.A. Maximov^{109,c},
 R. Mazini¹⁵¹, S.M. Mazza^{91a,91b}, G. Mc Goldrick¹⁵⁸, S.P. Mc Kee⁸⁹, A. McCarn⁸⁹, R.L. McCarthy¹⁴⁸,
 T.G. McCarthy²⁹, N.A. McCubbin¹³¹, K.W. McFarlane^{56,*}, J.A. McFayden⁷⁸, G. Mchedlidze⁵⁴,
 S.J. McMahon¹³¹, R.A. McPherson^{169,k}, M. Medinnis⁴², S. Meehan^{145a}, S. Mehlhase¹⁰⁰, A. Mehta⁷⁴,
 K. Meier^{58a}, C. Meineck¹⁰⁰, B. Meirose⁴¹, B.R. Mellado Garcia^{145c}, F. Meloni¹⁷, A. Mengarelli^{20a,20b},
 S. Menke¹⁰¹, E. Meoni¹⁶¹, K.M. Mercurio⁵⁷, S. Mergelmeyer²¹, P. Mermod⁴⁹, L. Merola^{104a,104b},
 C. Meroni^{91a}, F.S. Merritt³¹, A. Messina^{132a,132b}, J. Metcalfe²⁵, A.S. Mete¹⁶³, C. Meyer⁸³, C. Meyer¹²²,
 J-P. Meyer¹³⁶, J. Meyer¹⁰⁷, H. Meyer Zu Theenhausen^{58a}, R.P. Middleton¹³¹, S. Miglioranza^{164a,164c},
 L. Mijović²¹, G. Mikenberg¹⁷², M. Mikestikova¹²⁷, M. Mikuž⁷⁵, M. Milesi⁸⁸, A. Milic³⁰, D.W. Miller³¹,
 C. Mills⁴⁶, A. Milov¹⁷², D.A. Milstead^{146a,146b}, A.A. Minaenko¹³⁰, Y. Minami¹⁵⁵, I.A. Minashvili⁶⁵,
 A.I. Mincer¹¹⁰, B. Mindur^{38a}, M. Mineev⁶⁵, Y. Ming¹⁷³, L.M. Mir¹², K.P. Mistry¹²², T. Mitani¹⁷¹,
 J. Mitrevski¹⁰⁰, V.A. Mitsou¹⁶⁷, A. Miucci⁴⁹, P.S. Miyagawa¹³⁹, J.U. Mjörnmark⁸¹, T. Moa^{146a,146b},
 K. Mochizuki⁸⁵, S. Mohapatra³⁵, W. Mohr⁴⁸, S. Molander^{146a,146b}, R. Moles-Valls²¹, R. Monden⁶⁸,
 K. Mönig⁴², C. Monini⁵⁵, J. Monk³⁶, E. Monnier⁸⁵, A. Montalbano¹⁴⁸, J. Montejo Berlingen¹²,
 F. Monticelli⁷¹, S. Monzani^{132a,132b}, R.W. Moore³, N. Morange¹¹⁷, D. Moreno¹⁶², M. Moreno Llácer⁵⁴,
 P. Morettini^{50a}, D. Mori¹⁴², T. Mori¹⁵⁵, M. Morii⁵⁷, M. Morinaga¹⁵⁵, V. Morisbak¹¹⁹, S. Moritz⁸³,
 A.K. Morley¹⁵⁰, G. Mornacchi³⁰, J.D. Morris⁷⁶, S.S. Mortensen³⁶, A. Morton⁵³, L. Morvaj¹⁰³,
 M. Mosidze^{51b}, J. Moss¹⁴³, K. Motohashi¹⁵⁷, R. Mount¹⁴³, E. Mountricha²⁵, S.V. Mouraviev^{96,*},
 E.J.W. Moyse⁸⁶, S. Muanza⁸⁵, R.D. Mudd¹⁸, F. Mueller¹⁰¹, J. Mueller¹²⁵, R.S.P. Mueller¹⁰⁰, T. Mueller²⁸,
 D. Muenstermann⁴⁹, P. Mullen⁵³, G.A. Mullier¹⁷, J.A. Murillo Quijada¹⁸, W.J. Murray^{170,131},
 H. Musheghyan⁵⁴, E. Musto¹⁵², A.G. Myagkov^{130,ac}, M. Myska¹²⁸, B.P. Nachman¹⁴³, O. Nackenhorst⁵⁴,
 J. Nadal⁵⁴, K. Nagai¹²⁰, R. Nagai¹⁵⁷, Y. Nagai⁸⁵, K. Nagano⁶⁶, A. Nagarkar¹¹¹, Y. Nagasaka⁵⁹,
 K. Nagata¹⁶⁰, M. Nagel¹⁰¹, E. Nagy⁸⁵, A.M. Nairz³⁰, Y. Nakahama³⁰, K. Nakamura⁶⁶, T. Nakamura¹⁵⁵,

I. Nakano ¹¹², H. Namasivayam ⁴¹, R.F. Naranjo Garcia ⁴², R. Narayan ³¹, D.I. Narrias Villar ^{58a},
T. Naumann ⁴², G. Navarro ¹⁶², R. Nayyar ⁷, H.A. Neal ⁸⁹, P.Yu. Nechaeva ⁹⁶, T.J. Neep ⁸⁴, P.D. Nef ¹⁴³,
A. Negri ^{121a,121b}, M. Negrini ^{20a}, S. Nektarijevic ¹⁰⁶, C. Nellist ¹¹⁷, A. Nelson ¹⁶³, S. Nemecek ¹²⁷,
P. Nemethy ¹¹⁰, A.A. Nepomuceno ^{24a}, M. Nessi ^{30,ad}, M.S. Neubauer ¹⁶⁵, M. Neumann ¹⁷⁵, R.M. Neves ¹¹⁰,
P. Nevski ²⁵, P.R. Newman ¹⁸, D.H. Nguyen ⁶, R.B. Nickerson ¹²⁰, R. Nicolaidou ¹³⁶, B. Nicquevert ³⁰,
J. Nielsen ¹³⁷, N. Nikiforou ³⁵, A. Nikiforov ¹⁶, V. Nikolaenko ^{130,ac}, I. Nikolic-Audit ⁸⁰, K. Nikolopoulos ¹⁸,
J.K. Nilsen ¹¹⁹, P. Nilsson ²⁵, Y. Ninomiya ¹⁵⁵, A. Nisati ^{132a}, R. Nisius ¹⁰¹, T. Nobe ¹⁵⁵, M. Nomachi ¹¹⁸,
I. Nomidis ²⁹, T. Nooney ⁷⁶, S. Norberg ¹¹³, M. Nordberg ³⁰, O. Novgorodova ⁴⁴, S. Nowak ¹⁰¹, M. Nozaki ⁶⁶,
L. Nozka ¹¹⁵, K. Ntekas ¹⁰, G. Nunes Hanninger ⁸⁸, T. Nunnemann ¹⁰⁰, E. Nurse ⁷⁸, F. Nuti ⁸⁸, B.J. O'Brien ⁴⁶,
F. O'grady ⁷, D.C. O'Neil ¹⁴², V. O'Shea ⁵³, F.G. Oakham ^{29,d}, H. Oberlack ¹⁰¹, T. Obermann ²¹, J. Ocariz ⁸⁰,
A. Ochi ⁶⁷, I. Ochoa ³⁵, J.P. Ochoa-Ricoux ^{32a}, S. Oda ⁷⁰, S. Odaka ⁶⁶, H. Ogren ⁶¹, A. Oh ⁸⁴, S.H. Oh ⁴⁵,
C.C. Ohm ¹⁵, H. Ohman ¹⁶⁶, H. Oide ³⁰, W. Okamura ¹¹⁸, H. Okawa ¹⁶⁰, Y. Okumura ³¹, T. Okuyama ⁶⁶,
A. Olariu ^{26b}, S.A. Olivares Pino ⁴⁶, D. Oliveira Damazio ²⁵, A. Olszewski ³⁹, J. Olszowska ³⁹,
A. Onofre ^{126a,126e}, K. Onogi ¹⁰³, P.U.E. Onyisi ^{31,s}, C.J. Oram ^{159a}, M.J. Oreglia ³¹, Y. Oren ¹⁵³,
D. Orestano ^{134a,134b}, N. Orlando ¹⁵⁴, C. Oropeza Barrera ⁵³, R.S. Orr ¹⁵⁸, B. Osculati ^{50a,50b}, R. Ospanov ⁸⁴,
G. Otero y Garzon ²⁷, H. Otono ⁷⁰, M. Ouchrif ^{135d}, F. Ould-Saada ¹¹⁹, A. Ouraou ¹³⁶, K.P. Oussoren ¹⁰⁷,
Q. Ouyang ^{33a}, A. Ovcharova ¹⁵, M. Owen ⁵³, R.E. Owen ¹⁸, V.E. Ozcan ^{19a}, N. Ozturk ⁸, K. Pachal ¹⁴²,
A. Pacheco Pages ¹², C. Padilla Aranda ¹², M. Pagáčová ⁴⁸, S. Pagan Griso ¹⁵, E. Paganis ¹³⁹, F. Paige ²⁵,
P. Pais ⁸⁶, K. Pajchel ¹¹⁹, G. Palacino ^{159b}, S. Palestini ³⁰, M. Palka ^{38b}, D. Pallin ³⁴, A. Palma ^{126a,126b},
Y.B. Pan ¹⁷³, E. St. Panagiotopoulou ¹⁰, C.E. Pandini ⁸⁰, J.G. Panduro Vazquez ⁷⁷, P. Pani ^{146a,146b},
S. Panitkin ²⁵, D. Pantea ^{26b}, L. Paolozzi ⁴⁹, Th.D. Papadopoulou ¹⁰, K. Papageorgiou ¹⁵⁴, A. Paramonov ⁶,
D. Paredes Hernandez ¹⁵⁴, M.A. Parker ²⁸, K.A. Parker ¹³⁹, F. Parodi ^{50a,50b}, J.A. Parsons ³⁵, U. Parzefall ⁴⁸,
E. Pasqualucci ^{132a}, S. Passaggio ^{50a}, F. Pastore ^{134a,134b,*}, Fr. Pastore ⁷⁷, G. Pásztor ²⁹, S. Pataria ¹⁷⁵,
N.D. Patel ¹⁵⁰, J.R. Pater ⁸⁴, T. Pauly ³⁰, J. Pearce ¹⁶⁹, B. Pearson ¹¹³, L.E. Pedersen ³⁶, M. Pedersen ¹¹⁹,
S. Pedraza Lopez ¹⁶⁷, R. Pedro ^{126a,126b}, S.V. Peleganchuk ^{109,c}, D. Pelikan ¹⁶⁶, O. Penc ¹²⁷, C. Peng ^{33a},
H. Peng ^{33b}, B. Penning ³¹, J. Penwell ⁶¹, D.V. Perepelitsa ²⁵, E. Perez Codina ^{159a},
M.T. Pérez García-Estañ ¹⁶⁷, L. Perini ^{91a,91b}, H. Pernegger ³⁰, S. Perrella ^{104a,104b}, R. Peschke ⁴²,
V.D. Peshekhonov ⁶⁵, K. Peters ³⁰, R.F.Y. Peters ⁸⁴, B.A. Petersen ³⁰, T.C. Petersen ³⁶, E. Petit ⁴², A. Petridis ¹,
C. Petridou ¹⁵⁴, P. Petroff ¹¹⁷, E. Petrolo ^{132a}, F. Petrucci ^{134a,134b}, N.E. Pettersson ¹⁵⁷, R. Pezoa ^{32b},
P.W. Phillips ¹³¹, G. Piacquadio ¹⁴³, E. Pianori ¹⁷⁰, A. Picazio ⁴⁹, E. Piccaro ⁷⁶, M. Piccinini ^{20a,20b},
M.A. Pickering ¹²⁰, R. Piegaia ²⁷, D.T. Pignotti ¹¹¹, J.E. Pilcher ³¹, A.D. Pilkington ⁸⁴, A.W.J. Pin ⁸⁴,
J. Pina ^{126a,126b,126d}, M. Pinamonti ^{164a,164c,ae}, J.L. Pinfold ³, A. Pingel ³⁶, S. Pires ⁸⁰, H. Pirumov ⁴²,
M. Pitt ¹⁷², C. Pizio ^{91a,91b}, L. Plazak ^{144a}, M.-A. Pleier ²⁵, V. Pleskot ¹²⁹, E. Plotnikova ⁶⁵,
P. Plucinski ^{146a,146b}, D. Pluth ⁶⁴, R. Poettgen ^{146a,146b}, L. Poggioli ¹¹⁷, D. Pohl ²¹, G. Polesello ^{121a},
A. Poley ⁴², A. Policicchio ^{37a,37b}, R. Polifka ¹⁵⁸, A. Polini ^{20a}, C.S. Pollard ⁵³, V. Polychronakos ²⁵,
K. Pommès ³⁰, L. Pontecorvo ^{132a}, B.G. Pope ⁹⁰, G.A. Popeneciu ^{26c}, D.S. Popovic ¹³, A. Poppleton ³⁰,
S. Pospisil ¹²⁸, K. Potamianos ¹⁵, I.N. Potrap ⁶⁵, C.J. Potter ¹⁴⁹, C.T. Potter ¹¹⁶, G. Poulard ³⁰, J. Poveda ³⁰,
V. Pozdnyakov ⁶⁵, P. Pralavorio ⁸⁵, A. Pranko ¹⁵, S. Prasad ³⁰, S. Prell ⁶⁴, D. Price ⁸⁴, L.E. Price ⁶,
M. Primavera ^{73a}, S. Prince ⁸⁷, M. Proissl ⁴⁶, K. Prokofiev ^{60c}, F. Prokoshin ^{32b}, E. Protopapadaki ¹³⁶,
S. Protopopescu ²⁵, J. Proudfoot ⁶, M. Przybycien ^{38a}, E. Ptacek ¹¹⁶, D. Puddu ^{134a,134b}, E. Pueschel ⁸⁶,
D. Poldon ¹⁴⁸, M. Purohit ^{25,af}, P. Puzo ¹¹⁷, J. Qian ⁸⁹, G. Qin ⁵³, Y. Qin ⁸⁴, A. Quadt ⁵⁴, D.R. Quarrie ¹⁵,
W.B. Quayle ^{164a,164b}, M. Queitsch-Maitland ⁸⁴, D. Quilty ⁵³, S. Raddum ¹¹⁹, V. Radeka ²⁵, V. Radescu ⁴²,
S.K. Radhakrishnan ¹⁴⁸, P. Radloff ¹¹⁶, P. Rados ⁸⁸, F. Ragusa ^{91a,91b}, G. Rahal ¹⁷⁸, S. Rajagopalan ²⁵,
M. Rammensee ³⁰, C. Rangel-Smith ¹⁶⁶, F. Rauscher ¹⁰⁰, S. Rave ⁸³, T. Ravenscroft ⁵³, M. Raymond ³⁰,
A.L. Read ¹¹⁹, N.P. Readioff ⁷⁴, D.M. Rebuffi ^{121a,121b}, A. Redelbach ¹⁷⁴, G. Redlinger ²⁵, R. Reece ¹³⁷,
K. Reeves ⁴¹, L. Rehnisch ¹⁶, J. Reichert ¹²², H. Reisin ²⁷, C. Rembser ³⁰, H. Ren ^{33a}, A. Renaud ¹¹⁷,
M. Rescigno ^{132a}, S. Resconi ^{91a}, O.L. Rezanova ^{109,c}, P. Reznicek ¹²⁹, R. Rezvani ⁹⁵, R. Richter ¹⁰¹,
S. Richter ⁷⁸, E. Richter-Was ^{38b}, O. Ricken ²¹, M. Ridel ⁸⁰, P. Rieck ¹⁶, C.J. Riegel ¹⁷⁵, J. Rieger ⁵⁴, O. Rifki ¹¹³,
M. Rijssenbeek ¹⁴⁸, A. Rimoldi ^{121a,121b}, L. Rinaldi ^{20a}, B. Ristić ⁴⁹, E. Ritsch ³⁰, I. Riu ¹², F. Rizatdinova ¹¹⁴,
E. Rizvi ⁷⁶, S.H. Robertson ^{87,k}, A. Robichaud-Veronneau ⁸⁷, D. Robinson ²⁸, J.E.M. Robinson ⁴²,
A. Robson ⁵³, C. Roda ^{124a,124b}, S. Roe ³⁰, O. Røhne ¹¹⁹, S. Rolli ¹⁶¹, A. Romaniouk ⁹⁸, M. Romano ^{20a,20b},
S.M. Romano Saez ³⁴, E. Romero Adam ¹⁶⁷, N. Rompotis ¹³⁸, M. Ronzani ⁴⁸, L. Roos ⁸⁰, E. Ros ¹⁶⁷,

S. Rosati ^{132a}, K. Rosbach ⁴⁸, P. Rose ¹³⁷, P.L. Rosendahl ¹⁴, O. Rosenthal ¹⁴¹, V. Rossetti ^{146a,146b},
E. Rossi ^{104a,104b}, L.P. Rossi ^{50a}, J.H.N. Rosten ²⁸, R. Rosten ¹³⁸, M. Rotaru ^{26b}, I. Roth ¹⁷², J. Rothberg ¹³⁸,
D. Rousseau ¹¹⁷, C.R. Royon ¹³⁶, A. Rozanov ⁸⁵, Y. Rozen ¹⁵², X. Ruan ^{145c}, F. Rubbo ¹⁴³, I. Rubinskiy ⁴²,
V.I. Rud ⁹⁹, C. Rudolph ⁴⁴, M.S. Rudolph ¹⁵⁸, F. Rühr ⁴⁸, A. Ruiz-Martinez ³⁰, Z. Rurikova ⁴⁸,
N.A. Rusakovich ⁶⁵, A. Ruschke ¹⁰⁰, H.L. Russell ¹³⁸, J.P. Rutherford ⁷, N. Ruthmann ³⁰, Y.F. Ryabov ¹²³,
M. Rybar ¹⁶⁵, G. Rybkin ¹¹⁷, N.C. Ryder ¹²⁰, A.F. Saavedra ¹⁵⁰, G. Sabato ¹⁰⁷, S. Sacerdoti ²⁷, A. Saddique ³,
H.F-W. Sadrozinski ¹³⁷, R. Sadykov ⁶⁵, F. Safai Tehrani ^{132a}, P. Saha ¹⁰⁸, M. Sahinsoy ^{58a}, M. Saimpert ¹³⁶,
T. Saito ¹⁵⁵, H. Sakamoto ¹⁵⁵, Y. Sakurai ¹⁷¹, G. Salamanna ^{134a,134b}, A. Salamon ^{133a}, J.E. Salazar Loyola ^{32b},
M. Saleem ¹¹³, D. Salek ¹⁰⁷, P.H. Sales De Bruin ¹³⁸, D. Salihagic ¹⁰¹, A. Salnikov ¹⁴³, J. Salt ¹⁶⁷,
D. Salvatore ^{37a,37b}, F. Salvatore ¹⁴⁹, A. Salvucci ^{60a}, A. Salzburger ³⁰, D. Sammel ⁴⁸, D. Sampsonidis ¹⁵⁴,
A. Sanchez ^{104a,104b}, J. Sánchez ¹⁶⁷, V. Sanchez Martinez ¹⁶⁷, H. Sandaker ¹¹⁹, R.L. Sandbach ⁷⁶,
H.G. Sander ⁸³, M.P. Sanders ¹⁰⁰, M. Sandhoff ¹⁷⁵, C. Sandoval ¹⁶², R. Sandstroem ¹⁰¹, D.P.C. Sankey ¹³¹,
M. Sannino ^{50a,50b}, A. Sansoni ⁴⁷, C. Santoni ³⁴, R. Santonico ^{133a,133b}, H. Santos ^{126a}, I. Santoyo Castillo ¹⁴⁹,
K. Sapp ¹²⁵, A. Saponov ⁶⁵, J.G. Saraiva ^{126a,126d}, B. Sarrazin ²¹, O. Sasaki ⁶⁶, Y. Sasaki ¹⁵⁵, K. Sato ¹⁶⁰,
G. Sauvage ^{5,*}, E. Sauvan ⁵, G. Savage ⁷⁷, P. Savard ^{158,d}, C. Sawyer ¹³¹, L. Sawyer ^{79,n}, J. Saxon ³¹,
C. Sbarra ^{20a}, A. Sbrizzi ^{20a,20b}, T. Scanlon ⁷⁸, D.A. Scannicchio ¹⁶³, M. Scarcella ¹⁵⁰, V. Scarfone ^{37a,37b},
J. Schaarschmidt ¹⁷², P. Schacht ¹⁰¹, D. Schaefer ³⁰, R. Schaefer ⁴², J. Schaeffer ⁸³, S. Schaepe ²¹,
S. Schaetzel ^{58b}, U. Schäfer ⁸³, A.C. Schaffer ¹¹⁷, D. Schaile ¹⁰⁰, R.D. Schamberger ¹⁴⁸, V. Scharf ^{58a},
V.A. Schegelsky ¹²³, D. Scheirich ¹²⁹, M. Schernau ¹⁶³, C. Schiavi ^{50a,50b}, C. Schillo ⁴⁸, M. Schioppa ^{37a,37b},
S. Schlenker ³⁰, K. Schmieden ³⁰, C. Schmitt ⁸³, S. Schmitt ^{58b}, S. Schmitt ⁴², B. Schneider ^{159a},
Y.J. Schnellbach ⁷⁴, U. Schnoor ⁴⁴, L. Schoeffel ¹³⁶, A. Schoening ^{58b}, B.D. Schoenrock ⁹⁰, E. Schopf ²¹,
A.L.S. Schorlemmer ⁵⁴, M. Schott ⁸³, D. Schouten ^{159a}, J. Schovancova ⁸, S. Schramm ⁴⁹, M. Schreyer ¹⁷⁴,
N. Schuh ⁸³, M.J. Schultens ²¹, H.-C. Schultz-Coulon ^{58a}, H. Schulz ¹⁶, M. Schumacher ⁴⁸, B.A. Schumm ¹³⁷,
Ph. Schune ¹³⁶, C. Schwanenberger ⁸⁴, A. Schwartzman ¹⁴³, T.A. Schwarz ⁸⁹, Ph. Schwegler ¹⁰¹,
H. Schweiger ⁸⁴, Ph. Schwemling ¹³⁶, R. Schwienhorst ⁹⁰, J. Schwindling ¹³⁶, T. Schwindt ²¹, F.G. Sciacca ¹⁷,
E. Scifo ¹¹⁷, G. Sciolla ²³, F. Scuri ^{124a,124b}, F. Scutti ²¹, J. Searcy ⁸⁹, G. Sedov ⁴², E. Sedykh ¹²³, P. Seema ²¹,
S.C. Seidel ¹⁰⁵, A. Seiden ¹³⁷, F. Seifert ¹²⁸, J.M. Seixas ^{24a}, G. Sekhniaidze ^{104a}, K. Sekhon ⁸⁹, S.J. Sekula ⁴⁰,
D.M. Seliverstov ^{123,*}, N. Semprini-Cesari ^{20a,20b}, C. Serfon ³⁰, L. Serin ¹¹⁷, L. Serkin ^{164a,164b}, T. Serre ⁸⁵,
M. Sessa ^{134a,134b}, R. Seuster ^{159a}, H. Severini ¹¹³, T. Sfiligoj ⁷⁵, F. Sforza ³⁰, A. Sfyrla ³⁰, E. Shabalina ⁵⁴,
M. Shamim ¹¹⁶, L.Y. Shan ^{33a}, R. Shang ¹⁶⁵, J.T. Shank ²², M. Shapiro ¹⁵, P.B. Shatalov ⁹⁷, K. Shaw ^{164a,164b},
S.M. Shaw ⁸⁴, A. Shcherbakova ^{146a,146b}, C.Y. Shehu ¹⁴⁹, P. Sherwood ⁷⁸, L. Shi ^{151,ag}, S. Shimizu ⁶⁷,
C.O. Shimmin ¹⁶³, M. Shimojima ¹⁰², M. Shiyakova ⁶⁵, A. Shmeleva ⁹⁶, D. Shoaleh Saadi ⁹⁵, M.J. Shochet ³¹,
S. Shojaii ^{91a,91b}, S. Shrestha ¹¹¹, E. Shulga ⁹⁸, M.A. Shupe ⁷, S. Shushkevich ⁴², P. Sicho ¹²⁷, P.E. Sidebo ¹⁴⁷,
O. Sidiropoulou ¹⁷⁴, D. Sidorov ¹¹⁴, A. Sidoti ^{20a,20b}, F. Siegert ⁴⁴, Dj. Sijacki ¹³, J. Silva ^{126a,126d}, Y. Silver ¹⁵³,
S.B. Silverstein ^{146a}, V. Simak ¹²⁸, O. Simard ⁵, Lj. Simic ¹³, S. Simion ¹¹⁷, E. Simioni ⁸³, B. Simmons ⁷⁸,
D. Simon ³⁴, P. Sinervo ¹⁵⁸, N.B. Sinev ¹¹⁶, M. Sioli ^{20a,20b}, G. Siragusa ¹⁷⁴, A.N. Sisakyan ^{65,*},
S.Yu. Sivoklokov ⁹⁹, J. Sjölin ^{146a,146b}, T.B. Sjursen ¹⁴, M.B. Skinner ⁷², H.P. Skottowe ⁵⁷, P. Skubic ¹¹³,
M. Slater ¹⁸, T. Slavicek ¹²⁸, M. Slawinska ¹⁰⁷, K. Sliwa ¹⁶¹, V. Smakhtin ¹⁷², B.H. Smart ⁴⁶, L. Smestad ¹⁴,
S.Yu. Smirnov ⁹⁸, Y. Smirnov ⁹⁸, L.N. Smirnova ^{99,ah}, O. Smirnova ⁸¹, M.N.K. Smith ³⁵, R.W. Smith ³⁵,
M. Smizanska ⁷², K. Smolek ¹²⁸, A.A. Snesarev ⁹⁶, G. Snidero ⁷⁶, S. Snyder ²⁵, R. Sobie ^{169,k}, F. Socher ⁴⁴,
A. Soffer ¹⁵³, D.A. Soh ^{151,ag}, G. Sokhrannyi ⁷⁵, C.A. Solans ³⁰, M. Solar ¹²⁸, J. Solc ¹²⁸, E.Yu. Soldatov ⁹⁸,
U. Soldevila ¹⁶⁷, A.A. Solodkov ¹³⁰, A. Soloshenko ⁶⁵, O.V. Solovyanov ¹³⁰, V. Solovyev ¹²³, P. Sommer ⁴⁸,
H.Y. Song ^{33b,y}, N. Soni ¹, A. Sood ¹⁵, A. Sopczak ¹²⁸, B. Sopko ¹²⁸, V. Sopko ¹²⁸, V. Sorin ¹², D. Sosa ^{58b},
M. Sosebee ⁸, C.L. Sotiropoulou ^{124a,124b}, R. Soualah ^{164a,164c}, A.M. Soukharev ^{109,c}, D. South ⁴²,
B.C. Sowden ⁷⁷, S. Spagnolo ^{73a,73b}, M. Spalla ^{124a,124b}, M. Spangenberg ¹⁷⁰, F. Spanò ⁷⁷, W.R. Spearman ⁵⁷,
D. Sperlich ¹⁶, F. Spettel ¹⁰¹, R. Spighi ^{20a}, G. Spigo ³⁰, L.A. Spiller ⁸⁸, M. Spousta ¹²⁹, R.D. St. Denis ^{53,*},
A. Stabile ^{91a}, S. Staerz ⁴⁴, J. Stahlman ¹²², R. Stamen ^{58a}, S. Stamm ¹⁶, E. Stanecka ³⁹, C. Stanescu ^{134a},
M. Stanescu-Bellu ⁴², M.M. Stanitzki ⁴², S. Stapnes ¹¹⁹, E.A. Starchenko ¹³⁰, J. Stark ⁵⁵, P. Staroba ¹²⁷,
P. Starovoitov ^{58a}, R. Staszewski ³⁹, P. Steinberg ²⁵, B. Stelzer ¹⁴², H.J. Stelzer ³⁰, O. Stelzer-Chilton ^{159a},
H. Stenzel ⁵², G.A. Stewart ⁵³, J.A. Stillings ²¹, M.C. Stockton ⁸⁷, M. Stoebe ⁸⁷, G. Stoicea ^{26b}, P. Stolte ⁵⁴,
S. Stonjek ¹⁰¹, A.R. Stradling ⁸, A. Straessner ⁴⁴, M.E. Stramaglia ¹⁷, J. Strandberg ¹⁴⁷,
S. Strandberg ^{146a,146b}, A. Strandlie ¹¹⁹, E. Strauss ¹⁴³, M. Strauss ¹¹³, P. Strizenec ^{144b}, R. Ströhmer ¹⁷⁴,

D.M. Strom¹¹⁶, R. Stroynowski⁴⁰, A. Strubig¹⁰⁶, S.A. Stucci¹⁷, B. Stugu¹⁴, N.A. Styles⁴², D. Su¹⁴³,
 J. Su¹²⁵, R. Subramaniam⁷⁹, A. Succurro¹², S. Suchek^{58a}, Y. Sugaya¹¹⁸, M. Suk¹²⁸, V.V. Sulin⁹⁶,
 S. Sultansoy^{4c}, T. Sumida⁶⁸, S. Sun⁵⁷, X. Sun^{33a}, J.E. Sundermann⁴⁸, K. Suruliz¹⁴⁹, G. Susinno^{37a,37b},
 M.R. Sutton¹⁴⁹, S. Suzuki⁶⁶, M. Svatos¹²⁷, M. Swiatlowski¹⁴³, I. Sykora^{144a}, T. Sykora¹²⁹, D. Ta⁴⁸,
 C. Taccini^{134a,134b}, K. Tackmann⁴², J. Taenzer¹⁵⁸, A. Taffard¹⁶³, R. Tafirout^{159a}, N. Taiblum¹⁵³,
 H. Takai²⁵, R. Takashima⁶⁹, H. Takeda⁶⁷, T. Takeshita¹⁴⁰, Y. Takubo⁶⁶, M. Talby⁸⁵, A.A. Talyshev^{109,c},
 J.Y.C. Tam¹⁷⁴, K.G. Tan⁸⁸, J. Tanaka¹⁵⁵, R. Tanaka¹¹⁷, S. Tanaka⁶⁶, B.B. Tannenwald¹¹¹, N. Tannoury²¹,
 S. Tapia Araya^{32b}, S. Tapprogge⁸³, S. Tarem¹⁵², F. Tarrade²⁹, G.F. Tartarelli^{91a}, P. Tas¹²⁹, M. Tasevsky¹²⁷,
 T. Tashiro⁶⁸, E. Tassi^{37a,37b}, A. Tavares Delgado^{126a,126b}, Y. Tayalati^{135d}, F.E. Taylor⁹⁴, G.N. Taylor⁸⁸,
 P.T.E. Taylor⁸⁸, W. Taylor^{159b}, F.A. Teischinger³⁰, M. Teixeira Dias Castanheira⁷⁶, P. Teixeira-Dias⁷⁷,
 K.K. Temming⁴⁸, D. Temple¹⁴², H. Ten Kate³⁰, P.K. Teng¹⁵¹, J.J. Teoh¹¹⁸, F. Tepel¹⁷⁵, S. Terada⁶⁶,
 K. Terashi¹⁵⁵, J. Terron⁸², S. Terzo¹⁰¹, M. Testa⁴⁷, R.J. Teuscher^{158,k}, T. Theveneaux-Pelzer³⁴,
 J.P. Thomas¹⁸, J. Thomas-Wilsker⁷⁷, E.N. Thompson³⁵, P.D. Thompson¹⁸, R.J. Thompson⁸⁴,
 A.S. Thompson⁵³, L.A. Thomsen¹⁷⁶, E. Thomson¹²², M. Thomson²⁸, R.P. Thun^{89,*}, M.J. Tibbetts¹⁵,
 R.E. Tice Torres⁸⁵, V.O. Tikhomirov^{96,ai}, Yu.A. Tikhonov^{109,c}, S. Timoshenko⁹⁸, E. Tiouchichine⁸⁵,
 P. Tipton¹⁷⁶, S. Tisserant⁸⁵, K. Todome¹⁵⁷, T. Todorov^{5,*}, S. Todorova-Nova¹²⁹, J. Tojo⁷⁰, S. Tokár^{144a},
 K. Tokushuku⁶⁶, K. Tollefson⁹⁰, E. Tolley⁵⁷, L. Tomlinson⁸⁴, M. Tomoto¹⁰³, L. Tompkins^{143,aj},
 K. Toms¹⁰⁵, E. Torrence¹¹⁶, H. Torres¹⁴², E. Torró Pastor¹³⁸, J. Toth^{85,ak}, F. Touchard⁸⁵, D.R. Tovey¹³⁹,
 T. Trefzger¹⁷⁴, L. Tremblet³⁰, A. Tricoli³⁰, I.M. Trigger^{159a}, S. Trincaz-Duvoid⁸⁰, M.F. Tripiana¹²,
 W. Trischuk¹⁵⁸, B. Trocmé⁵⁵, C. Troncon^{91a}, M. Trotter-McDonald¹⁵, M. Trovatelli¹⁶⁹, L. Truong^{164a,164c},
 M. Trzebinski³⁹, A. Trzupek³⁹, C. Tsarouchas³⁰, J.C.-L. Tseng¹²⁰, P.V. Tsiarshka⁹², D. Tsionou¹⁵⁴,
 G. Tsipolitis¹⁰, N. Tsirintanis⁹, S. Tsiskaridze¹², V. Tsiskaridze⁴⁸, E.G. Tskhadadze^{51a}, K.M. Tsui^{60a},
 I.I. Tsukerman⁹⁷, V. Tsulaia¹⁵, S. Tsuno⁶⁶, D. Tsybychev¹⁴⁸, A. Tudorache^{26b}, V. Tudorache^{26b},
 A.N. Tuna⁵⁷, S.A. Tupputi^{20a,20b}, S. Turchikhin^{99,ah}, D. Turecek¹²⁸, R. Turra^{91a,91b}, A.J. Turvey⁴⁰,
 P.M. Tuts³⁵, A. Tykhonov⁴⁹, M. Tylmad^{146a,146b}, M. Tyndel¹³¹, I. Ueda¹⁵⁵, R. Ueno²⁹,
 M. Ughetto^{146a,146b}, M. Uglund¹⁴, F. Ukegawa¹⁶⁰, G. Unal³⁰, A. Undrus²⁵, G. Unel¹⁶³, F.C. Ungaro⁴⁸,
 Y. Unno⁶⁶, C. Unverdorben¹⁰⁰, J. Urban^{144b}, P. Urquijo⁸⁸, P. Urrejola⁸³, G. Usai⁸, A. Usanova⁶²,
 L. Vacavant⁸⁵, V. Vacek¹²⁸, B. Vachon⁸⁷, C. Valderanis⁸³, N. Valencic¹⁰⁷, S. Valentinietti^{20a,20b},
 A. Valero¹⁶⁷, L. Valery¹², S. Valkar¹²⁹, S. Vallecorsa⁴⁹, J.A. Valls Ferrer¹⁶⁷, W. Van Den Wollenberg¹⁰⁷,
 P.C. Van Der Deijl¹⁰⁷, R. van der Geer¹⁰⁷, H. van der Graaf¹⁰⁷, N. van Eldik¹⁵², P. van Gemmeren⁶,
 J. Van Nieuwkoop¹⁴², I. van Vulpen¹⁰⁷, M.C. van Woerden³⁰, M. Vanadia^{132a,132b}, W. Vandelli³⁰,
 R. Vanguri¹²², A. Vaniachine⁶, F. Vannucci⁸⁰, G. Vardanyan¹⁷⁷, R. Vari^{132a}, E.W. Varnes⁷, T. Varol⁴⁰,
 D. Varouchas⁸⁰, A. Vartapetian⁸, K.E. Varvell¹⁵⁰, F. Vazeille³⁴, T. Vazquez Schroeder⁸⁷, J. Veatch⁷,
 L.M. Veloce¹⁵⁸, F. Veloso^{126a,126c}, T. Velz²¹, S. Veneziano^{132a}, A. Ventura^{73a,73b}, D. Ventura⁸⁶,
 M. Venturi¹⁶⁹, N. Venturi¹⁵⁸, A. Venturini²³, V. Vercesi^{121a}, M. Verducci^{132a,132b}, W. Verkerke¹⁰⁷,
 J.C. Vermeulen¹⁰⁷, A. Vest⁴⁴, M.C. Vetterli^{142,d}, O. Viazlo⁸¹, I. Vichou¹⁶⁵, T. Vickey¹³⁹,
 O.E. Vickey Boeriu¹³⁹, G.H.A. Viehhauser¹²⁰, S. Viel¹⁵, R. Vigne⁶², M. Villa^{20a,20b},
 M. Villaplana Perez^{91a,91b}, E. Vilucchi⁴⁷, M.G. Vincker²⁹, V.B. Vinogradov⁶⁵, I. Vivarelli¹⁴⁹,
 F. Vives Vaque³, S. Vlachos¹⁰, D. Vladoiu¹⁰⁰, M. Vlasak¹²⁸, M. Vogel^{32a}, P. Vokac¹²⁸, G. Volpi^{124a,124b},
 M. Volpi⁸⁸, H. von der Schmitt¹⁰¹, H. von Radziewski⁴⁸, E. von Toerne²¹, V. Vorobel¹²⁹, K. Vorobev⁹⁸,
 M. Vos¹⁶⁷, R. Voss³⁰, J.H. Vossebeld⁷⁴, N. Vranjes¹³, M. Vranjes Milosavljevic¹³, V. Vrba¹²⁷,
 M. Vreeswijk¹⁰⁷, R. Vuillermet³⁰, I. Vukotic³¹, Z. Vykydal¹²⁸, P. Wagner²¹, W. Wagner¹⁷⁵,
 H. Wahlberg⁷¹, S. Wahrenmund⁴⁴, J. Wakabayashi¹⁰³, J. Walder⁷², R. Walker¹⁰⁰, W. Walkowiak¹⁴¹,
 C. Wang¹⁵¹, F. Wang¹⁷³, H. Wang¹⁵, H. Wang⁴⁰, J. Wang⁴², J. Wang¹⁵⁰, K. Wang⁸⁷, R. Wang⁶,
 S.M. Wang¹⁵¹, T. Wang²¹, T. Wang³⁵, X. Wang¹⁷⁶, C. Wanotayaraj¹¹⁶, A. Warburton⁸⁷, C.P. Ward²⁸,
 D.R. Wardrope⁷⁸, A. Washbrook⁴⁶, C. Wasicki⁴², P.M. Watkins¹⁸, A.T. Watson¹⁸, I.J. Watson¹⁵⁰,
 M.F. Watson¹⁸, G. Watts¹³⁸, S. Watts⁸⁴, B.M. Waugh⁷⁸, S. Webb⁸⁴, M.S. Weber¹⁷, S.W. Weber¹⁷⁴,
 J.S. Webster³¹, A.R. Weidberg¹²⁰, B. Weinert⁶¹, J. Weingarten⁵⁴, C. Weiser⁴⁸, H. Weits¹⁰⁷, P.S. Wells³⁰,
 T. Wenaus²⁵, T. Wengler³⁰, S. Wenig³⁰, N. Wermes²¹, M. Werner⁴⁸, P. Werner³⁰, M. Wessels^{58a},
 J. Wetter¹⁶¹, K. Whalen¹¹⁶, A.M. Wharton⁷², A. White⁸, M.J. White¹, R. White^{32b}, S. White^{124a,124b},
 D. Whiteson¹⁶³, F.J. Wickens¹³¹, W. Wiedenmann¹⁷³, M. Wielers¹³¹, P. Wienemann²¹,
 C. Wigglesworth³⁶, L.A.M. Wiik-Fuchs²¹, A. Wildauer¹⁰¹, H.G. Wilkens³⁰, H.H. Williams¹²²,

S. Williams¹⁰⁷, C. Willis⁹⁰, S. Willocq⁸⁶, A. Wilson⁸⁹, J.A. Wilson¹⁸, I. Wingerter-Seez⁵, F. Winklmeier¹¹⁶, B.T. Winter²¹, M. Wittgen¹⁴³, J. Wittkowski¹⁰⁰, S.J. Wollstadt⁸³, M.W. Wolter³⁹, H. Wolters^{126a,126c}, B.K. Wosiek³⁹, J. Wotschack³⁰, M.J. Woudstra⁸⁴, K.W. Wozniak³⁹, M. Wu⁵⁵, M. Wu³¹, S.L. Wu¹⁷³, X. Wu⁴⁹, Y. Wu⁸⁹, T.R. Wyatt⁸⁴, B.M. Wynne⁴⁶, S. Xella³⁶, D. Xu^{33a}, L. Xu²⁵, B. Yabsley¹⁵⁰, S. Yacoob^{145a}, R. Yakabe⁶⁷, M. Yamada⁶⁶, D. Yamaguchi¹⁵⁷, Y. Yamaguchi¹¹⁸, A. Yamamoto⁶⁶, S. Yamamoto¹⁵⁵, T. Yamanaka¹⁵⁵, K. Yamauchi¹⁰³, Y. Yamazaki⁶⁷, Z. Yan²², H. Yang^{33e}, H. Yang¹⁷³, Y. Yang¹⁵¹, W.-M. Yao¹⁵, Y.C. Yap⁸⁰, Y. Yasu⁶⁶, E. Yatsenko⁵, K.H. Yau Wong²¹, J. Ye⁴⁰, S. Ye²⁵, I. Yeletsikh⁶⁵, A.L. Yen⁵⁷, E. Yildirim⁴², K. Yorita¹⁷¹, R. Yoshida⁶, K. Yoshihara¹²², C. Young¹⁴³, C.J.S. Young³⁰, S. Youssef²², D.R. Yu¹⁵, J. Yu⁸, J.M. Yu⁸⁹, J. Yu¹¹⁴, L. Yuan⁶⁷, S.P.Y. Yuen²¹, A. Yurkewicz¹⁰⁸, I. Yusuff^{28,al}, B. Zabinski³⁹, R. Zaidan⁶³, A.M. Zaitsev^{130,ac}, J. Zalieckas¹⁴, A. Zaman¹⁴⁸, S. Zambito⁵⁷, L. Zanello^{132a,132b}, D. Zanzi⁸⁸, C. Zeitnitz¹⁷⁵, M. Zeman¹²⁸, A. Zemla^{38a}, Q. Zeng¹⁴³, K. Zengel²³, O. Zenin¹³⁰, T. Ženiš^{144a}, D. Zerwas¹¹⁷, D. Zhang⁸⁹, F. Zhang¹⁷³, G. Zhang^{33b}, H. Zhang^{33c}, J. Zhang⁶, L. Zhang⁴⁸, R. Zhang^{33b,i}, X. Zhang^{33d}, Z. Zhang¹¹⁷, X. Zhao⁴⁰, Y. Zhao^{33d,117}, Z. Zhao^{33b}, A. Zhemchugov⁶⁵, J. Zhong¹²⁰, B. Zhou⁸⁹, C. Zhou⁴⁵, L. Zhou³⁵, L. Zhou⁴⁰, M. Zhou¹⁴⁸, N. Zhou^{33f}, C.G. Zhu^{33d}, H. Zhu^{33a}, J. Zhu⁸⁹, Y. Zhu^{33b}, X. Zhuang^{33a}, K. Zhukov⁹⁶, A. Zibell¹⁷⁴, D. Zieminska⁶¹, N.I. Zimine⁶⁵, C. Zimmermann⁸³, S. Zimmermann⁴⁸, Z. Zinonos⁵⁴, M. Zinser⁸³, M. Ziolkowski¹⁴¹, L. Živković¹³, G. Zobernig¹⁷³, A. Zoccoli^{20a,20b}, M. zur Nedden¹⁶, G. Zurzolo^{104a,104b}, L. Zwalinski³⁰

¹ Department of Physics, University of Adelaide, Adelaide, Australia

² Physics Department, SUNY Albany, Albany, NY, United States

³ Department of Physics, University of Alberta, Edmonton, AB, Canada

⁴ (a) Department of Physics, Ankara University, Ankara; (b) Istanbul Aydin University, Istanbul; (c) Division of Physics, TOBB University of Economics and Technology, Ankara, Turkey

⁵ LAPP, CNRS/IN2P3 and Université Savoie Mont Blanc, Annecy-le-Vieux, France

⁶ High Energy Physics Division, Argonne National Laboratory, Argonne, IL, United States

⁷ Department of Physics, University of Arizona, Tucson, AZ, United States

⁸ Department of Physics, The University of Texas at Arlington, Arlington, TX, United States

⁹ Physics Department, University of Athens, Athens, Greece

¹⁰ Physics Department, National Technical University of Athens, Zografou, Greece

¹¹ Institute of Physics, Azerbaijan Academy of Sciences, Baku, Azerbaijan

¹² Institut de Física d'Altes Energies and Departament de Física de la Universitat Autònoma de Barcelona, Barcelona, Spain

¹³ Institute of Physics, University of Belgrade, Belgrade, Serbia

¹⁴ Department for Physics and Technology, University of Bergen, Bergen, Norway

¹⁵ Physics Division, Lawrence Berkeley National Laboratory and University of California, Berkeley, CA, United States

¹⁶ Department of Physics, Humboldt University, Berlin, Germany

¹⁷ Albert Einstein Center for Fundamental Physics and Laboratory for High Energy Physics, University of Bern, Bern, Switzerland

¹⁸ School of Physics and Astronomy, University of Birmingham, Birmingham, United Kingdom

¹⁹ (a) Department of Physics, Bogazici University, Istanbul; (b) Department of Physics Engineering, Gaziantep University, Gaziantep; (c) Department of Physics, Dogus University, Istanbul, Turkey

²⁰ (a) INFN Sezione di Bologna; (b) Dipartimento di Fisica e Astronomia, Università di Bologna, Bologna, Italy

²¹ Physikalisches Institut, University of Bonn, Bonn, Germany

²² Department of Physics, Boston University, Boston, MA, United States

²³ Department of Physics, Brandeis University, Waltham, MA, United States

²⁴ (a) Universidade Federal do Rio De Janeiro COPPE/EE/IF, Rio de Janeiro; (b) Electrical Circuits Department, Federal University of Juiz de Fora (UFJF), Juiz de Fora; (c) Federal University of Sao Joao del Rei (UFSJ), Sao Joao del Rei; (d) Instituto de Física, Universidade de Sao Paulo, Sao Paulo, Brazil

²⁵ Physics Department, Brookhaven National Laboratory, Upton, NY, United States

²⁶ (a) Transilvania University of Brasov, Brasov; (b) National Institute of Physics and Nuclear Engineering, Bucharest; (c) National Institute for Research and Development of Isotopic and Molecular Technologies, Physics Department, Cluj Napoca; (d) University Politehnica Bucharest, Bucharest; (e) West University in Timisoara, Timisoara, Romania

²⁷ Departamento de Física, Universidad de Buenos Aires, Buenos Aires, Argentina

²⁸ Cavendish Laboratory, University of Cambridge, Cambridge, United Kingdom

²⁹ Department of Physics, Carleton University, Ottawa, ON, Canada

³⁰ CERN, Geneva, Switzerland

³¹ Enrico Fermi Institute, University of Chicago, Chicago, IL, United States

³² (a) Departamento de Física, Pontificia Universidad Católica de Chile, Santiago; (b) Departamento de Física, Universidad Técnica Federico Santa María, Valparaíso, Chile

³³ (a) Institute of High Energy Physics, Chinese Academy of Sciences, Beijing; (b) Department of Modern Physics, University of Science and Technology of China, Anhui; (c) Department of Physics, Nanjing University, Jiangsu; (d) School of Physics, Shandong University, Shandong; (e) Department of Physics and Astronomy, Shanghai Key Laboratory for Particle Physics and Cosmology, Shanghai Jiao Tong University, Shanghai; (f) Physics Department, Tsinghua University, Beijing 100084, China

³⁴ Laboratoire de Physique Corpusculaire, Clermont Université and Université Blaise Pascal and CNRS/IN2P3, Clermont-Ferrand, France

³⁵ Nevis Laboratory, Columbia University, Irvington, NY, United States

³⁶ Niels Bohr Institute, University of Copenhagen, Copenhagen, Denmark

³⁷ (a) INFN Gruppo Collegato di Cosenza, Laboratori Nazionali di Frascati; (b) Dipartimento di Fisica, Università della Calabria, Rende, Italy

³⁸ (a) AGH University of Science and Technology, Faculty of Physics and Applied Computer Science, Krakow; (b) Marian Smoluchowski Institute of Physics, Jagiellonian University, Krakow, Poland

³⁹ Institute of Nuclear Physics Polish Academy of Sciences, Krakow, Poland

⁴⁰ Physics Department, Southern Methodist University, Dallas, TX, United States

⁴¹ Physics Department, University of Texas at Dallas, Richardson, TX, United States

⁴² DESY, Hamburg and Zeuthen, Germany

⁴³ Institut für Experimentelle Physik IV, Technische Universität Dortmund, Dortmund, Germany

⁴⁴ Institut für Kern- und Teilchenphysik, Technische Universität Dresden, Dresden, Germany

⁴⁵ Department of Physics, Duke University, Durham, NC, United States

⁴⁶ SUPA – School of Physics and Astronomy, University of Edinburgh, Edinburgh, United Kingdom

⁴⁷ INFN Laboratori Nazionali di Frascati, Frascati, Italy

- 48 Fakultät für Mathematik und Physik, Albert-Ludwigs-Universität, Freiburg, Germany
- 49 Section de Physique, Université de Genève, Geneva, Switzerland
- 50 (a) INFN Sezione di Genova; (b) Dipartimento di Fisica, Università di Genova, Genova, Italy
- 51 (a) E. Andronikashvili Institute of Physics, Iv. Javakishvili Tbilisi State University, Tbilisi; (b) High Energy Physics Institute, Tbilisi State University, Tbilisi, Georgia
- 52 II Physikalisches Institut, Justus-Liebig-Universität Giessen, Giessen, Germany
- 53 SUPA – School of Physics and Astronomy, University of Glasgow, Glasgow, United Kingdom
- 54 II Physikalisches Institut, Georg-August-Universität, Göttingen, Germany
- 55 Laboratoire de Physique Subatomique et de Cosmologie, Université Grenoble-Alpes, CNRS/IN2P3, Grenoble, France
- 56 Department of Physics, Hampton University, Hampton, VA, United States
- 57 Laboratory for Particle Physics and Cosmology, Harvard University, Cambridge, MA, United States
- 58 (a) Kirchhoff-Institut für Physik, Ruprecht-Karls-Universität Heidelberg, Heidelberg; (b) Physikalisches Institut, Ruprecht-Karls-Universität Heidelberg, Heidelberg; (c) ZITI Institut für technische Informatik, Ruprecht-Karls-Universität Heidelberg, Mannheim, Germany
- 59 Faculty of Applied Information Science, Hiroshima Institute of Technology, Hiroshima, Japan
- 60 (a) Department of Physics, The Chinese University of Hong Kong, Shatin, N.T., Hong Kong; (b) Department of Physics, The University of Hong Kong, Hong Kong; (c) Department of Physics, The Hong Kong University of Science and Technology, Clear Water Bay, Kowloon, Hong Kong, China
- 61 Department of Physics, Indiana University, Bloomington, IN, United States
- 62 Institut für Astro- und Teilchenphysik, Leopold-Franzens-Universität, Innsbruck, Austria
- 63 University of Iowa, Iowa City, IA, United States
- 64 Department of Physics and Astronomy, Iowa State University, Ames, IA, United States
- 65 Joint Institute for Nuclear Research, JINR Dubna, Dubna, Russia
- 66 KEK, High Energy Accelerator Research Organization, Tsukuba, Japan
- 67 Graduate School of Science, Kobe University, Kobe, Japan
- 68 Faculty of Science, Kyoto University, Kyoto, Japan
- 69 Kyoto University of Education, Kyoto, Japan
- 70 Department of Physics, Kyushu University, Fukuoka, Japan
- 71 Instituto de Física La Plata, Universidad Nacional de La Plata and CONICET, La Plata, Argentina
- 72 Physics Department, Lancaster University, Lancaster, United Kingdom
- 73 (a) INFN Sezione di Lecce; (b) Dipartimento di Matematica e Fisica, Università del Salento, Lecce, Italy
- 74 Oliver Lodge Laboratory, University of Liverpool, Liverpool, United Kingdom
- 75 Department of Physics, Jožef Stefan Institute and University of Ljubljana, Ljubljana, Slovenia
- 76 School of Physics and Astronomy, Queen Mary University of London, London, United Kingdom
- 77 Department of Physics, Royal Holloway University of London, Surrey, United Kingdom
- 78 Department of Physics and Astronomy, University College London, London, United Kingdom
- 79 Louisiana Tech University, Ruston, LA, United States
- 80 Laboratoire de Physique Nucléaire et de Hautes Energies, UPMC and Université Paris-Diderot and CNRS/IN2P3, Paris, France
- 81 Fysiska institutionen, Lunds universitet, Lund, Sweden
- 82 Departamento de Física Teórica C-15, Universidad Autónoma de Madrid, Madrid, Spain
- 83 Institut für Physik, Universität Mainz, Mainz, Germany
- 84 School of Physics and Astronomy, University of Manchester, Manchester, United Kingdom
- 85 CPPM, Aix-Marseille Université and CNRS/IN2P3, Marseille, France
- 86 Department of Physics, University of Massachusetts, Amherst, MA, United States
- 87 Department of Physics, McGill University, Montreal, QC, Canada
- 88 School of Physics, University of Melbourne, Victoria, Australia
- 89 Department of Physics, The University of Michigan, Ann Arbor, MI, United States
- 90 Department of Physics and Astronomy, Michigan State University, East Lansing, MI, United States
- 91 (a) INFN Sezione di Milano; (b) Dipartimento di Fisica, Università di Milano, Milano, Italy
- 92 B.I. Stepanov Institute of Physics, National Academy of Sciences of Belarus, Minsk, Republic of Belarus
- 93 National Scientific and Educational Centre for Particle and High Energy Physics, Minsk, Republic of Belarus
- 94 Department of Physics, Massachusetts Institute of Technology, Cambridge, MA, United States
- 95 Group of Particle Physics, University of Montreal, Montreal, QC, Canada
- 96 P.N. Lebedev Institute of Physics, Academy of Sciences, Moscow, Russia
- 97 Institute for Theoretical and Experimental Physics (ITEP), Moscow, Russia
- 98 National Research Nuclear University MEPhI, Moscow, Russia
- 99 D.V. Skobel'syn Institute of Nuclear Physics, M.V. Lomonosov Moscow State University, Moscow, Russia
- 100 Fakultät für Physik, Ludwig-Maximilians-Universität München, München, Germany
- 101 Max-Planck-Institut für Physik (Werner-Heisenberg-Institut), München, Germany
- 102 Nagasaki Institute of Applied Science, Nagasaki, Japan
- 103 Graduate School of Science and Kobayashi-Maskawa Institute, Nagoya University, Nagoya, Japan
- 104 (a) INFN Sezione di Napoli; (b) Dipartimento di Fisica, Università di Napoli, Napoli, Italy
- 105 Department of Physics and Astronomy, University of New Mexico, Albuquerque, NM, United States
- 106 Institute for Mathematics, Astrophysics and Particle Physics, Radboud University Nijmegen/Nikhef, Nijmegen, Netherlands
- 107 Nikhef National Institute for Subatomic Physics and University of Amsterdam, Amsterdam, Netherlands
- 108 Department of Physics, Northern Illinois University, DeKalb, IL, United States
- 109 Budker Institute of Nuclear Physics, SB RAS, Novosibirsk, Russia
- 110 Department of Physics, New York University, New York, NY, United States
- 111 Ohio State University, Columbus, OH, United States
- 112 Faculty of Science, Okayama University, Okayama, Japan
- 113 Homer L. Dodge Department of Physics and Astronomy, University of Oklahoma, Norman, OK, United States
- 114 Department of Physics, Oklahoma State University, Stillwater, OK, United States
- 115 Palacký University, RCPTM, Olomouc, Czech Republic
- 116 Center for High Energy Physics, University of Oregon, Eugene, OR, United States
- 117 LAL, Université Paris-Sud and CNRS/IN2P3, Orsay, France
- 118 Graduate School of Science, Osaka University, Osaka, Japan
- 119 Department of Physics, University of Oslo, Oslo, Norway
- 120 Department of Physics, Oxford University, Oxford, United Kingdom
- 121 (a) INFN Sezione di Pavia; (b) Dipartimento di Fisica, Università di Pavia, Pavia, Italy
- 122 Department of Physics, University of Pennsylvania, Philadelphia, PA, United States
- 123 National Research Centre "Kurchatov Institute" B.P. Konstantinov Petersburg Nuclear Physics Institute, St. Petersburg, Russia
- 124 (a) INFN Sezione di Pisa; (b) Dipartimento di Fisica E. Fermi, Università di Pisa, Pisa, Italy

- ¹²⁵ Department of Physics and Astronomy, University of Pittsburgh, Pittsburgh, PA, United States
- ¹²⁶ ^(a) Laboratório de Instrumentação e Física Experimental de Partículas – LIP, Lisboa; ^(b) Faculdade de Ciências, Universidade de Lisboa, Lisboa; ^(c) Department of Physics, University of Coimbra, Coimbra; ^(d) Centro de Física Nuclear da Universidade de Lisboa, Lisboa; ^(e) Departamento de Física, Universidade do Minho, Braga; ^(f) Departamento de Física Teórica y del Cosmos and CAFPE, Universidad de Granada, Granada (Spain); ^(g) Dep Física and CEFITEC of Faculdade de Ciências e Tecnologia, Universidade Nova de Lisboa, Caparica, Portugal
- ¹²⁷ Institute of Physics, Academy of Sciences of the Czech Republic, Praha, Czech Republic
- ¹²⁸ Czech Technical University in Prague, Praha, Czech Republic
- ¹²⁹ Faculty of Mathematics and Physics, Charles University in Prague, Praha, Czech Republic
- ¹³⁰ State Research Center Institute for High Energy Physics (Protvino), NRC KI, Russia
- ¹³¹ Particle Physics Department, Rutherford Appleton Laboratory, Didcot, United Kingdom
- ¹³² ^(a) INFN Sezione di Roma; ^(b) Dipartimento di Fisica, Sapienza Università di Roma, Roma, Italy
- ¹³³ ^(a) INFN Sezione di Roma Tor Vergata; ^(b) Dipartimento di Fisica, Università di Roma Tor Vergata, Roma, Italy
- ¹³⁴ ^(a) INFN Sezione di Roma Tre; ^(b) Dipartimento di Matematica e Fisica, Università Roma Tre, Roma, Italy
- ¹³⁵ ^(a) Faculté des Sciences Ain Chock, Réseau Universitaire de Physique des Hautes Energies – Université Hassan II, Casablanca; ^(b) Centre National de l’Energie des Sciences Techniques Nucleaires, Rabat; ^(c) Faculté des Sciences Semlalia, Université Cadi Ayyad, LPHEA, Marrakech; ^(d) Faculté des Sciences, Université Mohamed Premier and LPTPM, Oujda; ^(e) Faculté des sciences, Université Mohammed V, Rabat, Morocco
- ¹³⁶ DSM/IRFU (Institut de Recherches sur les Lois Fondamentales de l’Univers), CEA Saclay (Commissariat à l’Energie Atomique et aux Energies Alternatives), Gif-sur-Yvette, France
- ¹³⁷ Santa Cruz Institute for Particle Physics, University of California Santa Cruz, Santa Cruz, CA, United States
- ¹³⁸ Department of Physics, University of Washington, Seattle, WA, United States
- ¹³⁹ Department of Physics and Astronomy, University of Sheffield, Sheffield, United Kingdom
- ¹⁴⁰ Department of Physics, Shinshu University, Nagano, Japan
- ¹⁴¹ Fachbereich Physik, Universität Siegen, Siegen, Germany
- ¹⁴² Department of Physics, Simon Fraser University, Burnaby, BC, Canada
- ¹⁴³ SLAC National Accelerator Laboratory, Stanford, CA, United States
- ¹⁴⁴ ^(a) Faculty of Mathematics, Physics & Informatics, Comenius University, Bratislava; ^(b) Department of Subnuclear Physics, Institute of Experimental Physics of the Slovak Academy of Sciences, Kosice, Slovak Republic
- ¹⁴⁵ ^(a) Department of Physics, University of Cape Town, Cape Town; ^(b) Department of Physics, University of Johannesburg, Johannesburg; ^(c) School of Physics, University of the Witwatersrand, Johannesburg, South Africa
- ¹⁴⁶ ^(a) Department of Physics, Stockholm University; ^(b) The Oskar Klein Centre, Stockholm, Sweden
- ¹⁴⁷ Physics Department, Royal Institute of Technology, Stockholm, Sweden
- ¹⁴⁸ Departments of Physics & Astronomy and Chemistry, Stony Brook University, Stony Brook, NY, United States
- ¹⁴⁹ Department of Physics and Astronomy, University of Sussex, Brighton, United Kingdom
- ¹⁵⁰ School of Physics, University of Sydney, Sydney, Australia
- ¹⁵¹ Institute of Physics, Academia Sinica, Taipei, Taiwan
- ¹⁵² Department of Physics, Technion: Israel Institute of Technology, Haifa, Israel
- ¹⁵³ Raymond and Beverly Sackler School of Physics and Astronomy, Tel Aviv University, Tel Aviv, Israel
- ¹⁵⁴ Department of Physics, Aristotle University of Thessaloniki, Thessaloniki, Greece
- ¹⁵⁵ International Center for Elementary Particle Physics and Department of Physics, The University of Tokyo, Tokyo, Japan
- ¹⁵⁶ Graduate School of Science and Technology, Tokyo Metropolitan University, Tokyo, Japan
- ¹⁵⁷ Department of Physics, Tokyo Institute of Technology, Tokyo, Japan
- ¹⁵⁸ Department of Physics, University of Toronto, Toronto, ON, Canada
- ¹⁵⁹ ^(a) TRIUMF, Vancouver, BC; ^(b) Department of Physics and Astronomy, York University, Toronto, ON, Canada
- ¹⁶⁰ Faculty of Pure and Applied Sciences, and Center for Integrated Research in Fundamental Science and Engineering, University of Tsukuba, Tsukuba, Japan
- ¹⁶¹ Department of Physics and Astronomy, Tufts University, Medford, MA, United States
- ¹⁶² Centro de Investigaciones, Universidad Antonio Narino, Bogota, Colombia
- ¹⁶³ Department of Physics and Astronomy, University of California Irvine, Irvine, CA, United States
- ¹⁶⁴ ^(a) INFN Gruppo Collegato di Udine, Sezione di Trieste, Udine; ^(b) ICTP, Trieste; ^(c) Dipartimento di Chimica, Fisica e Ambiente, Università di Udine, Udine, Italy
- ¹⁶⁵ Department of Physics, University of Illinois, Urbana, IL, United States
- ¹⁶⁶ Department of Physics and Astronomy, University of Uppsala, Uppsala, Sweden
- ¹⁶⁷ Instituto de Física Corpuscular (IFIC) and Departamento de Física Atómica, Molecular y Nuclear and Departamento de Ingeniería Electrónica and Instituto de Microelectrónica de Barcelona (IMB-CNM), University of Valencia and CSIC, Valencia, Spain
- ¹⁶⁸ Department of Physics, University of British Columbia, Vancouver, BC, Canada
- ¹⁶⁹ Department of Physics and Astronomy, University of Victoria, Victoria, BC, Canada
- ¹⁷⁰ Department of Physics, University of Warwick, Coventry, United Kingdom
- ¹⁷¹ Waseda University, Tokyo, Japan
- ¹⁷² Department of Particle Physics, The Weizmann Institute of Science, Rehovot, Israel
- ¹⁷³ Department of Physics, University of Wisconsin, Madison, WI, United States
- ¹⁷⁴ Fakultät für Physik und Astronomie, Julius-Maximilians-Universität, Würzburg, Germany
- ¹⁷⁵ Fachbereich C Physik, Bergische Universität Wuppertal, Wuppertal, Germany
- ¹⁷⁶ Department of Physics, Yale University, New Haven, CT, United States
- ¹⁷⁷ Yerevan Physics Institute, Yerevan, Armenia
- ¹⁷⁸ Centre de Calcul de l’Institut National de Physique Nucléaire et de Physique des Particules (IN2P3), Villeurbanne, France

^a Also at Department of Physics, King’s College London, London, United Kingdom.

^b Also at Institute of Physics, Azerbaijan Academy of Sciences, Baku, Azerbaijan.

^c Also at Novosibirsk State University, Novosibirsk, Russia.

^d Also at TRIUMF, Vancouver, BC, Canada.

^e Also at Department of Physics, California State University, Fresno, CA, United States.

^f Also at Department of Physics, University of Fribourg, Fribourg, Switzerland.

^g Also at Departamento de Física e Astronomia, Faculdade de Ciências, Universidade do Porto, Portugal.

^h Also at Tomsk State University, Tomsk, Russia.

ⁱ Also at CPPM, Aix-Marseille Université and CNRS/IN2P3, Marseille, France.

^j Also at Università di Napoli Parthenope, Napoli, Italy.

^k Also at Institute of Particle Physics (IPP), Canada.

^l Also at Particle Physics Department, Rutherford Appleton Laboratory, Didcot, United Kingdom.

^m Also at Department of Physics, St. Petersburg State Polytechnical University, St. Petersburg, Russia.

ⁿ Also at Louisiana Tech University, Ruston, LA, United States.

^o Also at Institutio Catalana de Recerca i Estudis Avancats, ICREA, Barcelona, Spain.

- ^p Also at Department of Physics, The University of Michigan, Ann Arbor, MI, United States.
- ^q Also at Graduate School of Science, Osaka University, Osaka, Japan.
- ^r Also at Department of Physics, National Tsing Hua University, Taiwan.
- ^s Also at Department of Physics, The University of Texas at Austin, Austin, TX, United States.
- ^t Also at Institute of Theoretical Physics, Iliia State University, Tbilisi, Georgia.
- ^u Also at CERN, Geneva, Switzerland.
- ^v Also at Georgian Technical University (GTU), Tbilisi, Georgia.
- ^w Also at Manhattan College, New York, NY, United States.
- ^x Also at Hellenic Open University, Patras, Greece.
- ^y Also at Institute of Physics, Academia Sinica, Taipei, Taiwan.
- ^z Also at LAL, Université Paris-Sud and CNRS/IN2P3, Orsay, France.
- ^{aa} Also at Academia Sinica Grid Computing, Institute of Physics, Academia Sinica, Taipei, Taiwan.
- ^{ab} Also at School of Physics, Shandong University, Shandong, China.
- ^{ac} Also at Moscow Institute of Physics and Technology State University, Dolgoprudny, Russia.
- ^{ad} Also at Section de Physique, Université de Genève, Geneva, Switzerland.
- ^{ae} Also at International School for Advanced Studies (SISSA), Trieste, Italy.
- ^{af} Also at Department of Physics and Astronomy, University of South Carolina, Columbia, SC, United States.
- ^{ag} Also at School of Physics and Engineering, Sun Yat-sen University, Guangzhou, China.
- ^{ah} Also at Faculty of Physics, M.V. Lomonosov Moscow State University, Moscow, Russia.
- ^{ai} Also at National Research Nuclear University MEPhI, Moscow, Russia.
- ^{aj} Also at Department of Physics, Stanford University, Stanford, CA, United States.
- ^{ak} Also at Institute for Particle and Nuclear Physics, Wigner Research Centre for Physics, Budapest, Hungary.
- ^{al} Also at University of Malaya, Department of Physics, Kuala Lumpur, Malaysia.
- * Deceased.